

INTEGER SUPERHARMONIC MATRICES ON THE F -LATTICE

AHMED BOU-RABEE

ABSTRACT. We prove that the set of quadratic growths achievable by integer superharmonic functions on the F -lattice, a periodic subgraph of \mathbb{Z}^2 with oriented edges, has the structure of an overlapping circle packing. The proof recursively constructs a distinct pair of recurrent functions for each rational point on a hyperbola. This resolves a conjecture of Smart (2013) and characterizes the scaling limit of the Abelian sandpile on the F -lattice.

1. INTRODUCTION

The F -lattice is a directed, periodic, planar graph (\mathbb{Z}^2, E) , where

$$\begin{cases} (x \pm e_1, x) \in E & \text{if } x_1 + x_2 \pmod{2} = 0 \\ (x \pm e_2, x) \in E & \text{otherwise,} \end{cases}$$

and e_1, e_2 are the standard basis vectors in \mathbb{Z}^2 . A function $g : \mathbb{Z}^2 \rightarrow \mathbb{Z}$ is *integer superharmonic* if

$$(1) \quad \Delta g(x) := \sum_{(y,x) \in E} (g(y) - g(x)) \leq 0,$$

for all $x \in \mathbb{Z}^2$. Let S_2 denote the set of 2×2 symmetric matrices. The *quadratic growth* of g is specified by $A \in S_2$,

$$(2) \quad g(x) = \frac{1}{2}x \cdot Ax + o(1 + |x|^2).$$

When g is integer superharmonic and has quadratic growth A , we say that it is an *integer superharmonic representative* of A and A is an *integer superharmonic matrix*. Moreover, g is *recurrent* if whenever $f : \mathbb{Z}^2 \rightarrow \mathbb{Z}$ is integer superharmonic and $X \subset \mathbb{Z}^2$ is finite and strongly connected (with respect to E),

$$(3) \quad \sup_X (g - f) \leq \sup_{\partial X} (g - f),$$

where $\partial X = \{y \in \mathbb{Z}^2 : \text{there is } x \in X \text{ with } (y, x) \in E\}$. We call an integer superharmonic representative of A which is recurrent an *odometer* for A .

In this article we demonstrate an explicit characterization of integer superharmonic matrices on the F -lattice via a recursive construction of their odometers.

1.1. Background. Any periodic Euclidean directed graph, (V, E) , defines a set of integer superharmonic matrices. The study of these matrices was initiated by Pegden and Smart [PS13] in the context of the Abelian sandpile model of Bak, Tang and Wiesenfeld and Dhar [BTW87, Dha90]. We briefly describe the model, referring the interested reader to the surveys [Red05, HLM⁺08, Jár18] and books [Kli18, CP18].



FIGURE 1. A 5×5 section of the F -lattice

The Abelian sandpile is a diffusion process on (V, E) , of which the following, the *single-source sandpile*, is a canonical example. Start with n chips at the origin (or the closest point to the origin) in V . When a vertex has at least as many chips as outgoing edges, it topples, sending one chip along each outgoing edge. When n is large, the final configuration of chips, $s_n : V \rightarrow \mathbb{Z}$, displays fascinating fractal structure. Pegden-Smart made it possible to study this structure by showing that s_n converges weakly-* to a limiting $s : \mathbb{R}^d \rightarrow \mathbb{R}$ which is described by the solution to a certain nonlinear partial differentiable equation, later called the *sandpile PDE*.

The sandpile PDE is characterized by the set of integer superharmonic matrices on (V, E) ; in particular, the fractal structure of large sandpiles is dependent on the graph upon which the sandpile is run. In a tour de force, Levine, Pegden, and Smart showed that the set of integer superharmonic matrices on the square lattice, \mathbb{Z}^2 with nearest neighbor edges, is the downwards closure of an Apollonian circle packing [LPS17]. This led to an understanding of the fractal patterns appearing in sandpile experiments, [LPS16, PS20], something which had evaded physicists and mathematicians for decades [LKG90, LBR02, Ost03].

Levine-Pegden-Smart's proof in [LPS17] involved explicitly constructing an odometer for each circle in an Apollonian band packing. Their construction mirrored the recursive generation of Apollonian circle packings - it pieced together later odometers from earlier ones. Our strategy in this article is similar but with several key differences which we detail in Section 2.

The patterns which appear in s_n on the F -lattice have also been investigated by mathematical physicists with notable contributions made by Caracciolo, Paoletti, and Sportiello [CPS08, Pao12] and Dhar, Sadhu, Chandra [DSC09, DS13, DS10, DS11]. This article provides a new perspective on their results. For example, the patterns which appear in their experiments correspond empirically to the two Laplacians of the 'peak' and 'valley' odometers. In fact, an immediate consequence of Theorems 1.1 and 1.2 is that the weak-* limit of the sandpile identity on ellipsoidal domains is constant [Mel20]. We leave open, but expect that these results can also be used to construct more elaborate sandpile fractals as in [LPS16]. Moreover, it is a difficult open problem to construct the weak-* limit of the single-source sandpile on the square lattice. It would be interesting to see if the simple structure of the sandpile PDE here can be used to make progress on this for the F -lattice.



FIGURE 2. A few periods of the bases of cones in $\partial\Gamma_F$.

1.2. Main results. Our primary result is that the set of integer superharmonic matrices on the F -lattice is the downwards closure of an overlapping circle packing.

Theorem 1.1. *$A \in S_2$ is integer superharmonic if and only if the difference*

$$\frac{1}{2} \begin{bmatrix} s-t & s+t \\ s+t & t-s \end{bmatrix} - A$$

is positive semidefinite for some $s, t \in \mathbb{Z}$.

We explain the connection to circles. Denote the set of integer superharmonic matrices on the F -lattice by Γ_F . The boundary of Γ_F may be viewed as a surface by taking the parameterization $M : S_2 \rightarrow \mathbb{R}^3$,

$$M(a, b, c) := \frac{1}{2} \begin{bmatrix} c+a & b \\ b & c-a \end{bmatrix}.$$

In particular, Theorem 1.1 may be restated as

$$\partial\Gamma_F = \{M(a, b, \gamma_F(a, b)) : (a, b) \in \mathbb{R}^2\},$$

where

$$(4) \quad \gamma(x)_F := \max_{s, t \in \mathbb{Z}} -|x - (s - t, s + t)|.$$

Viewed from above, $\partial\Gamma_F$ is the union of identical slope-1 cones whose bases are the overlapping circle packing displayed in Figure 2.

One may check that the matrices, $M(s - t, s + t, 0)$ lie on $\partial\Gamma_F$ for all $s, t \in \mathbb{Z}$ (see Section 1.3 for the data to do so in a more general setting). This together with the downwards closure of Γ_F reduces the proof of Theorem 1.1 to verifying that the intersection curve of each pair of overlapping cones is in $\partial\Gamma_F$. Moreover, by symmetry, it suffices to check only one such hyperbola. Smart made these observations in [Sma13] and then conjectured the following, which we prove.

Theorem 1.2. *For each $0 \leq t \leq 1$, $M(t, 1 - t, -\sqrt{t^2 + (1 - t)^2})$ lies on the boundary of Γ_F .*



FIGURE 3. The first three iterations of a hyperbola recursion defined in Section 3. The two visible hyperbolas are outlined by dashed lines.

The set Γ_F is closed (Lemma 3.4 in [LPS17]), therefore, it suffices to prove Theorem 1.2 for all rational $0 \leq t \leq 1$ along the bottom branch of the hyperbola $\mathcal{H} := \{(t, c) \in \mathbb{R} \times \mathbb{R}^- : t^2 + (1-t)^2 = c^2\}$. We do this recursively. We start with explicit formulas for the odometers for $(0, -1)$ and $(1, -1)$ and then use those to construct odometers for all other rational points in between. Surprisingly, the recursion requires building not just one odometer for each such rational t , but *two* distinct odometers. This is a significant difference between the square lattice case which builds one odometer at a time; the square lattice odometers were also later shown to have a strong uniqueness property [PS20].

Another new challenge is in identifying the correct recursive structure. There is a well-known secant line sweep algorithm which produces (and parameterizes) the rational points on \mathcal{H} given a single rational point on \mathcal{H} (and generally any elliptic curve - see *e.g.* [Tan96]). For example, since $(0, -1) \in \mathcal{H}$, all other rational points can be enumerated by varying the rational slope of a secant line between $(0, -1)$ and \mathcal{H} . Unfortunately, the odometers lying on \mathcal{H} under this labeling do not have an apparent recursive structure.

The parameterization which we adopt in this article utilizes the geometry of two adjacent cones. Each rational point on \mathcal{H} is an intersection of two unique lines of rational slope starting at the apexes of the cones. These intersections are dense in \mathcal{H} so we may identify each such point by its rational slope. See Figure 3.

Specifically, each point in $\mathbb{Q}^2 \cap \mathcal{H}$ may be labeled by a reduced fraction $0 \leq n/d \leq 1$ with corresponding matrix

$$(5) \quad M(n, d) := \frac{1}{(d^2 + 2dn - n^2)} \begin{bmatrix} -n^2 & dn \\ dn & -d^2 \end{bmatrix}.$$

We construct odometers for each $M(n, d)$ which grow along the lattice of the matrix,

$$(6) \quad L(n, d) = \{x \in \mathbb{Z}^2 : M(n, d) \cdot x \in \mathbb{Z}^2\},$$

and which have periodic Laplacians. However, the F -lattice is not transitive. In particular, if $h : \mathbb{Z}^2 \rightarrow \mathbb{Z}$ is $L(n, d)$ periodic, then Δh may not be $L(n, d)$ periodic unless its period is even. To circumvent this, we must pass to a sub-lattice by doubling along the kernel of



FIGURE 4. One $L'(2, 5)$ period of $\Delta g_{2,5}$ and $\Delta \hat{g}_{2,5}$. White and black are values of 0 and 1 respectively. These are used to construct the odometers seen in Figure 7.

$M(n, d)$. We show in Section 3 that $L(n, d)$ is equal to the integer span of

$$(7) \quad v_{n/d,1} := \begin{bmatrix} d \\ n \end{bmatrix} \quad v_{n/d,2} := \begin{bmatrix} n-d \\ n+d \end{bmatrix},$$

and $v_{n/d,1}$ generates the kernel of $M(n, d)$. Our modified lattice is

$$(8) \quad L'(n, d) = \begin{cases} L(n, d) & \text{if } (n+d) \text{ is even} \\ 2\mathbb{Z}v_{n/d,1} + \mathbb{Z}v_{n/d,2} & \text{if } (n+d) \text{ is odd.} \end{cases}$$

We then derive Theorem 1.2 from the following.

Theorem 1.3. *For each reduced fraction $0 < n/d < 1$ there exists two distinct odometers $g_{n,d}, \hat{g}_{n,d}$ both of which satisfy the periodicity condition,*

$$(9) \quad g(x+v) = g(x) + x^t M(n, d)x + c_v$$

for all $v \in L'(n, d)$.

As in [LPS17], the periodicity condition (9) implies that $g_{n,d}$ and $\hat{g}_{n,d}$ are each integer superharmonic representatives for $M(n, d)$. Moreover, integer superharmonic matrices with odometers are on $\partial\Gamma_F$. Indeed, if g were recurrent but not on the boundary of Γ_F there would exist an integer superharmonic $f \geq g + \delta|x|^2$ for some $\delta > 0$. However, on the boundary of a ball of radius n , B_n , $\sup_{\partial B_n}(g-f) \leq -n\delta/2^2$ for all n sufficiently large, contradicting the definition of recurrent as $\sup_{B_n}(g-f) \geq g(0) - f(0)$, a constant.

1.3. $F^{(k)}$ lattices and Kleian bugs. We briefly mention a connection and possible extensions of this work. The overlapping circle packing in Figure 2 is an example of an object recently coined as a *Kleian bug* [KK21]. Kleian bugs may be thought of as a generalization of Apollonian circle packings in which circles are allowed to have prescribed overlaps. In particular, the Apollonian band packing from [LPS17] is a Kleian bug. An important aspect of [LPS17] is an analogue of Descartes rule for integer superharmonic functions - Kleian bugs share a similar rule.

The symmetry group of the Kleian bug for the F -lattice is trivial (the difficult aspect of the argument in this manuscript is in accounting for the intersections between adjacent

cones). However, numerical evidence suggests that the set of integer superharmonic matrices on other planar lattices may also be described by nontrivial symmetries of Kleinian bugs.

Levine-Pegden-Smart have derived a numerical algorithm which can determine the set of integer superharmonic matrices on periodic graphs up to arbitrary precision [LPS16] (see [Peg] for some high resolution outputs of this algorithm). We ran the Levine-Pegden-Smart algorithm on a family of lattices which generalize the F -lattice, what we call the $F^{(k)}$ lattices. For each $k \geq 2$, the $F^{(k)}$ -lattice is a directed, periodic, planar graph $(\mathbb{Z}^2, E^{(k)})$, where

$$\begin{cases} (x \pm e_1, x) \in E & \text{if } x_1 + x_2 \pmod k = 0 \\ (x \pm e_2, x) \in E & \text{otherwise.} \end{cases}$$

Computed sets of $\partial\Gamma_k$, the boundary of the set of integer superharmonic matrices for the $F^{(k)}$ lattice, are in Figure 5.

Some basic structure of these sets for all $k \geq 2$ may be understood after verifying that

$$(10) \quad \begin{aligned} \Delta r_1(x, y) &= 1\{(x_1 + x_2) \pmod k \neq 0\} & \text{for } r_1(x_1, x_2) &= \frac{x_2(x_2 + 1)}{2} \\ \Delta r_2 &= \Delta r_1 & \text{for } r_2(x_1, x_2) &= q_k(x_1 + x_2) \\ \Delta r_3 &= 1 & \text{for } r_3(x_1, x_2) &= \frac{x_1(x_1 + 1) + x_2(x_2 + 1)}{2} \end{aligned}$$

where

$$q_k(n) = \frac{(k-1)}{2k}(n^2 - s^2) + \frac{s(s-1)}{2} \quad \text{where } s = n \pmod k,$$

(note the Laplacian is that of the $F^{(k)}$ lattice). In particular, $h_1 := r_1 - r_2$ is integer valued and harmonic, $\Delta h_1 = 0$. The function $h_2(x_1, x_2) = x_1 x_2$ is also harmonic. This together with (10) and the standard argument in Lemma 6.1 below can be used to show that $r_i + s \cdot h_1 + t \cdot h_2 - r_3$ are odometers for all $s, t \in \mathbb{Z}$ and $i \in \{1, 2\}$. These odometers lie on the hyperbolas between the largest cones in Figure 5 and the harmonic functions explain the apparent periodicity of Γ_k .

Remark 1. *Interestingly, the function $q_k(n)$ also counts the number of edges in a k -partite Turan graph of order n . We note that $q_k(n)$ has a simple closed form when k is small,*

$$q_k(n) = \lfloor \frac{(k-1)}{2k} n^2 \rfloor \quad \text{only for } k \leq 7,$$

but this is false for $k \geq 8$.

We have not been able to make progress in understanding Γ_k for $k \geq 3$ beyond (10). The general characterization of Γ_k seems to require both a recursive construction of the odometers for all circles in a Kleinian bug as in [LPS17] and all rational points on an infinite family of distinct hyperbolas. For example, we have explicitly computed in Figure 6 odometers for some of the largest circles appearing in $\partial\Gamma_3$. Each pair of overlapping circles generates a new hyperbola which we must check contains a dense family of odometers.

We leave the possibility of more detailed investigations of Γ_k for future work. From here onwards, we focus solely on Γ_2 and omit the sub/superscripts.

1.4. Supplementary materials. Code which produces tile odometers will be uploaded on the arXiv.

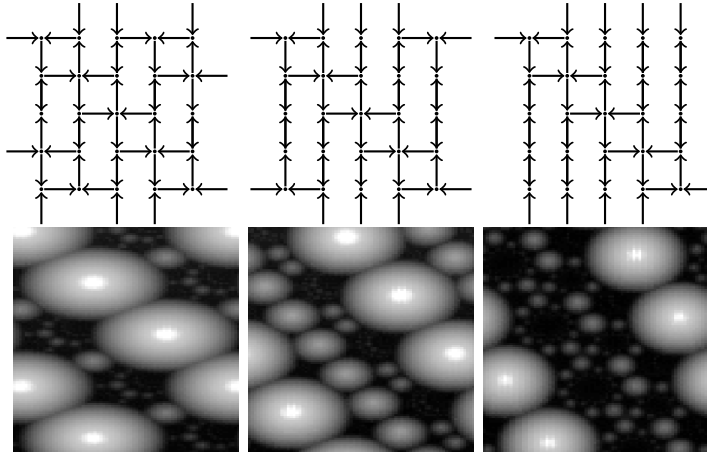


FIGURE 5. The $F^{(k)}$ lattices for $k = 3, 4, 5$ and computed $\partial\Gamma_k$.

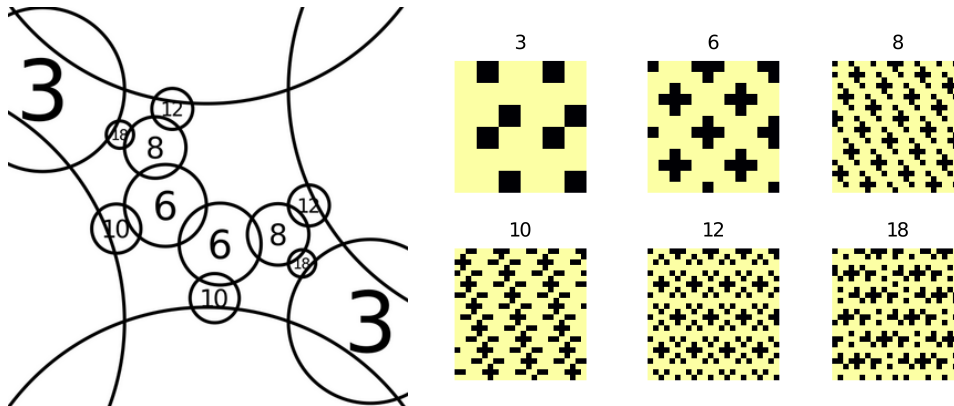


FIGURE 6. The seven largest circles in a period of $\partial\Gamma_3$. Periods of the Laplacians of odometers for the indicated circles on the left are displayed on the right, black is -1 and yellow is 0. Note that the four bordering largest circles have Laplacian identically 0 and correspond to harmonic functions built from (10).

Acknowledgments. Thank you to Charles K. Smart for valuable feedback throughout this project.

2. PROOF OUTLINE AND COMPARISON TO PREVIOUS WORK

Our method at a high level follows the outline of [LPS16]: the proof recursively constructs odometers which then identify Γ_F . The implementation of this outline, however, requires several new ideas, the most significant being the recursive algorithm itself.

In order to make the comparison, we briefly recall Levine-Pegden-Smart's construction in [LPS16]. On the square lattice, odometers were built by first specifying a *tile odometer*, a function with a finite domain, and then extending that function via a periodicity condition like (9) above. Levine-Pegden-Smart's construction associates tile odometers to circles in an Apollonian band packing. Recall that Apollonian packings can be drawn by starting with a triple of mutually tangent circles and then recursively filling in Soddy circles [GLM⁺05].

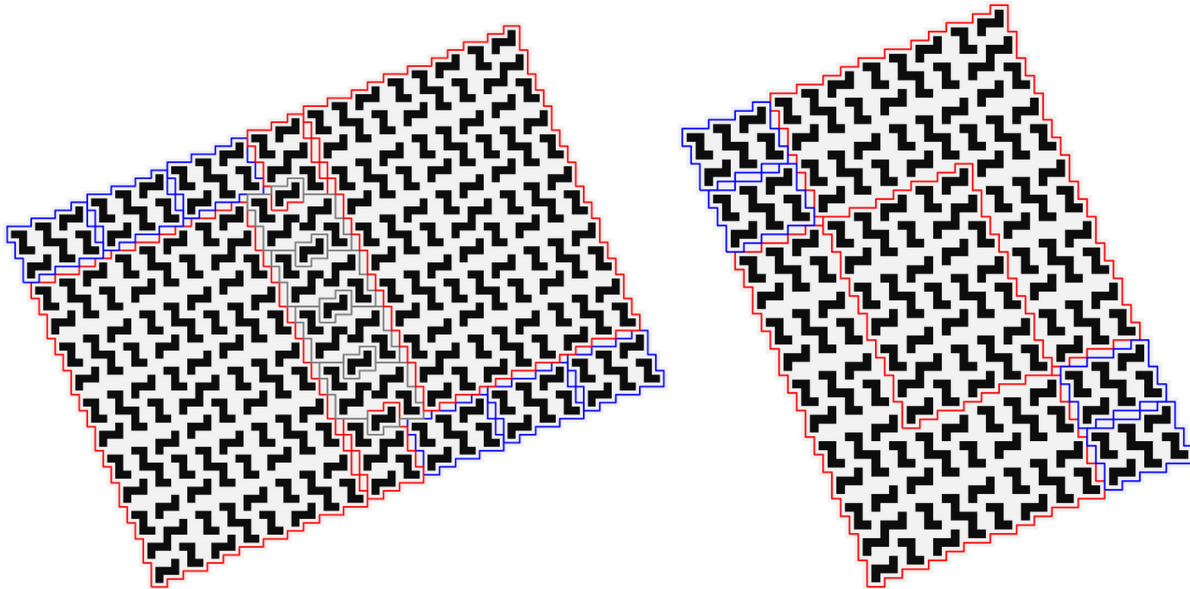


FIGURE 7. The Laplacian of two standard tile odometers corresponding to the Farey pair $(13/32, 15/37)$. Gray is 0 and black is -1. The Laplacian of the standard odd-even ancestor odometers and alternate odometers are outlined in blue, red, and gray respectively. On the right, the odometer decomposes perfectly into four-two copies of the odd-even standard odometers for the parent Farey pair, $(2/5, 11/27)$. In particular, two copies of the even parent overlap perfectly on a copy of an even grandparent. On the left, the odometer does not have a perfect decomposition into parents or grandparents; the decomposition requires multiple copies of the standard and alternate odometers of the distant ancestor pair $(2/5, 3/7)$.

Each circle in a packing is then part of a *Descartes quadruple* of pair-wise mutually tangent circles - thus every circle (other than the initial three) has a unique triple of parent circles. Levine-Pegden-Smart build tile odometers following this - the recursion starts with a simple formula for the largest circles in a band packing and then builds each child odometer by gluing together two copies each of the three parent odometers in a specified way.

In our setting, the Apollonian band packing is replaced by reduced rationals $0 \leq t \leq 1$ lying on a hyperbola $\mathcal{H} = \{(t, c) \in \mathbb{R} \times \mathbb{R}^+ : t^2 + (1-t)^2 = c^2\}$. The rational recursion is Farey-like but parity aware. That is, all *odd* and *even* reduced rationals - those whose numerator and denominator sum to an odd and even integer respectively - are grouped together into unique odd-even *Farey pairs*. The initial Farey pair is $(0/1, 1/1)$ and subsequent pairs are produced via a modification of the mediant operation and parent-child rotation; the rational recursion produces a ternary tree of unique *Farey quadruples*, a grouping of child and parent Farey pairs. We use this tree structure to recursively produce tile odometers.

A major difference beyond this is that we build for each reduced rational in a Farey pair not one but *two* distinct odometers. If the recursive algorithm attempted to use only one of the two odometers, it would get stuck - see Figure 7. (This can be thought of as coupling one odometer to each of the two intersecting downwards paths in Figure 3.) The construction also requires ancestor odometers which are arbitrarily far up the recursive tree. Moreover,

although the function domains, the *tiles*, constructed are 180-degree symmetric, the tile odometers are not even centrally symmetric, leading to a blow-up in the the number of cases the algorithm must consider.

For these reasons and more, proving correctness of the recursive algorithm presents new technical challenges. A notable one being distant ancestor dependence precludes a finite step inductive proof. We address this by augmenting the recursion and associating a binary *boundary string* to each odometer. These strings encapsulate certain compatibility properties across the recursive tree and show it is possible to glue distinct tile odometers together in a well-defined way.

Our proof that the functions which we construct are recurrent also differs from the corresponding proof on the square lattice. There, the odometers were shown to be *maximal*, a property strictly stronger than recurrent. The proof of maximality hinged on the fact that the Laplacians of the constructed odometers have a ‘web of 0s’, an infinite connected subgraph of 0s. In our case, there is no such web (which uses F -lattice edges) and no hyperbola odometer is maximal. Another technical difference is that the tiles which we construct do not tile \mathbb{Z}^2 - they ‘almost’ do and this is fortunately sufficient for our arguments.

To summarize, our proof proceeds as follows.

- (1) Identify a Farey-like recursion on reduced fractions $t = n/d$ which is dense on a hyperbola and tracks the parity of $(n + d)$.
- (2) Pair each reduced fraction with a binary word which records how it was generated.
- (3) Associate to each such word a *boundary string* which carries additional function and domain data.
- (4) Augment the rational recursion to produce two distinct tile odometers, a standard and an alternate by piecing together combinations of earlier standard and alternate odometers.
- (5) Show the recursion is well-defined by reducing every interface into a pair of boundary strings.
- (6) Prove that the functions constructed are recurrent and have the correct growth.

We start in Section 3 by precisely defining the modified Farey recursion on the hyperbola. We then prove a technical ‘almost’ tiling lemma in Section 4; this is later used to show that tile odometers extend periodically to cover space. Then in Section 5, we introduce and analyze a recursion on binary words which supplements the hyperbola recursion. There we also associate degenerate function and tile data, boundary strings, to each such word.

Then, in Section 6 we prove Theorem 1.3 for a special family of reduced fractions. In particular, this family is simple enough that we are able to provide explicit formulas for the tile odometers. This forms the base case for the general recursion. In Section 7 we then introduce a weak form of the recursion which essentially builds only the boundary of the tile odometers. We show that these boundaries consist of exactly the boundary strings from Section 5. The full recursion is completed in Section 8 where we show the interior of tile odometers can be filled in either by immediate parents or by a chain of distant ancestors. We conclude in Section 9 by showing that both standard and alternate tile odometers can be glued together in a way that give the desired growth and recurrence.

3. HYPERBOLA RECURSION

We specify a modified Farey recursion for rational matrices lying on the hyperbola $\mathcal{H} := \{(t, c) \in [0, 1] \times \mathbb{R}^- : t^2 + (1 - t)^2 = c^2\}$.

3.1. Matrix and lattice parameterization. Recall the map $M : S_2 \rightarrow \mathbb{R}^3$

$$(11) \quad M(a, b, c) = \frac{1}{2} \begin{bmatrix} c + a & b \\ b & c - a \end{bmatrix}$$

and the hyperbola matrices in the statement of Theorem 1.2, $M(t, 1 - t, -\sqrt{t^2 + (1 - t)^2})$. By solving for the intersection point of rank 1 perturbations of two adjacent cones and subtracting by a harmonic matrix, we can label $(t, c) \in \mathbb{Q} \cap \mathcal{H}$ by

$$(12) \quad f(n, d) := \frac{1}{T(n, d)} \cdot ((d^2 - n^2), -(d^2 + n^2)),$$

which has corresponding matrix

$$M(n, d) := \frac{1}{T(n, d)} \begin{bmatrix} -n^2 & dn \\ dn & -d^2 \end{bmatrix},$$

where $T(n, d) := (d^2 + 2dn - n^2)$. Another computation shows that $(n, d) \rightarrow (d - n, n + d)$ is a rotation along the hyperbola: $(a, b) \rightarrow (b, a)$. We will study these rotations in more depth in Section 3.3 once we have defined the rational recursion.

As indicated in the introduction, we consider the lattice

$$(13) \quad L'(n, d) = \begin{cases} \mathbb{Z}v_{n/d,1} + \mathbb{Z}v_{n/d,2} & \text{if } (n + d) \text{ is even} \\ 2\mathbb{Z}v_{n/d,1} + \mathbb{Z}v_{n/d,2} & \text{if } (n + d) \text{ is odd.} \end{cases}$$

where

$$(14) \quad v_{n/d,1} := \begin{bmatrix} d \\ n \end{bmatrix} \quad v_{n/d,2} := \begin{bmatrix} n - d \\ n + d \end{bmatrix}.$$

Setting $a_i := M(n, d) * v_i$, we note

$$(15) \quad a_1 := \begin{bmatrix} 0 \\ 0 \end{bmatrix} \quad a_2 := \begin{bmatrix} n \\ -d \end{bmatrix}.$$

We first observe that $v_{n/d,1}$ and $v_{n/d,2}$ generate the lattice of the matrix $M(n, d)$.

Lemma 3.1. *For each reduced fraction $t = n/d$,*

$$\{v \in \mathbb{Z}^2 : M(n, d) \cdot v \in \mathbb{Z}^2\} = \mathbb{Z}v_{n/d,1} + \mathbb{Z}v_{n/d,2}.$$

Proof. Suppose $M(n, d) \cdot x = y$ for $x, y \in \mathbb{Z}^2$. Since $\mathbb{R}^2 = \mathbb{R}v_1 + \mathbb{R}v_2$, we may write

$$x = cv_1 + c'v_2$$

for $c, c' \in \mathbb{Q}$. We show that c, c' must be in \mathbb{Z} , starting with c' . By (15),

$$M(n, d)x = cM(n, d) \cdot v_1 + c'M(n, d) \cdot v_2 = c'a_2$$

where by assumption

$$c'a_2 := \begin{bmatrix} z_1 \\ z_2 \end{bmatrix},$$

for integers z_1, z_2 . Since $\gcd(n, -d) = 1$, by Bezout's identity, there exists $d, d' \in \mathbb{Z}$ so that

$$dn - d'd = 1.$$

Multiplying the above expression by c' ,

$$dz_1 - d'z_2 = c',$$

in particular, since the left-hand side is integer-valued, $c' \in \mathbb{Z}$. Finally, since $x, v_1, v_2, c' \in \mathbb{Z}$, $cv_1 = x - c'v_2$ must also be integer-valued. The exact same argument then shows that $c \in \mathbb{Z}$. \square

We then check that the map in (12) is in fact dense in \mathcal{H} by noting it is dense in the first output.

Lemma 3.2. $\frac{d^2 - n^2}{d^2 + 2dn - n^2}$ is dense in $[0, 1]$ for reduced fractions $0 \leq n/d \leq 1$.

Proof. Suppose $0 < n/d < 1$ and rewrite

$$\frac{d^2 - n^2}{d^2 + 2dn - n^2} = 1 - \frac{1}{1 + \frac{1}{2}\left(\frac{d}{n} - \frac{n}{d}\right)}.$$

Conclude after observing that $\frac{d}{n} - \frac{n}{d}$ is dense in $[0, \infty)$. \square

3.2. Modified Farey recursion. As evident from (13), the recursion which we specify needs to be parity-aware. To that end, we say a reduced fraction p_n/p_d is *even* if $p_n + p_d$ is even and otherwise is *odd*. We exhibit a modified Farey recursion which generates all rationals in $[0, 1]$ and associates to each rational a unique set of odd-even parents and a sibling of the opposite parity.

An odd reduced fraction $p =: o_n/o_d$ and an even reduced fraction $q =: e_n/e_d$ produce an odd-even child pair by

$$(16) \quad \mathcal{C}(p, q) := \left(\frac{e_n + o_n}{e_d + o_d}, \frac{2 \cdot o_n + e_n}{2 \cdot o_d + e_d} \right).$$

A quadruple of reduced rationals, (p_1, q_1, p_2, q_2) is a *Farey quadruple* if $p_1, q_1 = \mathcal{C}(p_2, q_2)$, p_2 is odd, and q_2 is even. Each odd-even pair in a Farey quadruple is a *Farey pair*, the second pair are the *Farey parents* of each child in the first pair. A Farey quadruple (p_1, q_1, p_2, q_2) produces three children

$$(17) \quad \begin{array}{ll} \text{Type 1: } \mathcal{C}_1 & (\mathcal{C}(p_1, q_1), p_1, q_1) \\ \text{Type 2: } \mathcal{C}_2 & (\mathcal{C}(p_1, q_2), p_1, q_2) \\ \text{Type 3: } \mathcal{C}_3 & (\mathcal{C}(p_2, q_1), p_2, q_1). \end{array}$$

The *modified Farey recursion* begins with the base quadruple

$$(18) \quad \mathbf{q}_0 = \left(\frac{1}{2}, \frac{1}{3}, \frac{0}{1}, \frac{1}{1} \right),$$

and generates descendants which are labeled by words in the free monoid F_3^* generated by $\{1, 2, 3\}$. The empty word $\{\}$ corresponds to the base quadruple. Each letter in a word corresponds to the type of the child chosen in each step. For example $q_{(123)}$ refers to the quadruple taking the Type 1 child of the root, then the Type 2 child of that child, then the Type 3 child of that child.

Here is the connection to the usual, vanilla Farey recursion. Recall that the vanilla Farey sequence of order n consists of all reduced fractions of denominator at most n between 0 and 1. If a/b and c/d are neighboring terms in a vanilla Farey sequence of order n , then the first term which appears between them in a later sequence of order $m > n$ is the mediant, $p = \frac{a+c}{b+d}$. We refer to $(a/b, c/d)$ as the *vanilla Farey parents* of p while p is the *vanilla Farey child* of *vanilla Farey neighbors* $(a/b, c/d)$. We then observe that (16) is simply two steps of the vanilla Farey recursion.

Lemma 3.3. *The modified Farey recursion generates unique Farey quadruples in reduced form*

$$\mathbf{q} = (p_1, q_1, p_2, q_2) = \left(\frac{e_n + o_n}{e_d + o_d}, \frac{2 \cdot o_n + e_n}{2 \cdot o_d + e_d}, \frac{o_n}{o_d}, \frac{e_n}{e_d} \right),$$

in particular, p_1, p_2 are odd, q_1, q_2 are even and \mathbf{q} is a Farey quadruple.

Proof. This follows once we inductively check that (p_2, q_2) are vanilla Farey neighbors with vanilla Farey child p_1 and (p_1, p_2) are vanilla Farey neighbors with vanilla Farey child q_1 . That is, by induction, (p_1, q_1) , (p_1, q_2) , and (p_2, q_1) are each pairs of neighbors in some vanilla Farey sequence and thus each child has a unique set of Farey parents. \square

Lemma 3.3 shows that the recursion defines a ternary tree of Farey quadruples. Each node in the tree has 3 outgoing edges corresponding to the three types of children. For later reference let \mathcal{T}_n , denote the set of all Farey quadruples associated to words of length exactly n and denote the full tree by

$$(19) \quad \mathcal{T} = \bigcup \mathcal{T}_n.$$

3.3. Rotational symmetry reduction. As noted previously in Section 3.1, the following operator

$$(20) \quad \mathcal{R}(n, d) = (d - n, n + d)$$

rotates $\partial\Gamma_F$. The goal of this section is to show that an extension of \mathcal{R} to Farey quadruples preserves the depth of the modified Farey recursion. We start by observing a parity flipping property of \mathcal{R} .

Lemma 3.4. *If $0 \leq n/d \leq 1$ is an even reduced fraction then $\gcd((d - n)/2, (n + d)/2) = 1$, otherwise $\gcd(d - n, n + d) = 1$. Therefore, in the even case, the reduction of $\frac{d-n}{n+d}$ is odd and vice versa.*

Proof. We split the proof into two steps.

Step 1. We check the first claim. By the Euclidean algorithm,

$$\gcd(n, d) = \gcd(d - n, n) = 1,$$

and,

$$\begin{aligned} \gcd(n + d, d - n) &= \gcd((n + d) - (d - n), d - n) \\ &= \gcd(2n, d - n). \end{aligned}$$

If $(n+d)$ is even or odd, then $(d-n)$ is respectively even or odd. By Bezout's identity, there exist integers a_i, b_i so that

$$\begin{aligned} a_1(d-n) + b_1 2 &= c \\ a_2(d-n) + b_2 n &= 1 \end{aligned}$$

where c is 1 if $(d-n)$ is odd and 2 otherwise. Multiplying the above two expressions together shows that $\gcd(2n, d-n) = c$. If $c = 1$, we are done, otherwise, another application of Bezout's identity shows that there is a_3, b_3 so that

$$a_3(n+d) + b_3(d-n) = 2$$

and if we divide by 2 then

$$a_3(n+d)/2 + b_3(d-n)/2 = 1$$

which concludes this step.

Step 2. If $(n+d)$ is odd, then Step 1 shows $\frac{d-n}{d+n}$ is in reduced form and therefore is even. Otherwise, reduce $\frac{d-n}{d+n} = \frac{(d-n)/2}{(d+n)/2}$ and note $(d-n+d+n)/2 = d$. Since $(n+d)$ is even and $\gcd(n, d) = 1$, both n and d must be odd, concluding the proof. \square

In light of Lemma 3.4, we extend \mathcal{R} to act on reduced fractions n/d by:

$$(21) \quad \mathcal{R}(n, d) = \begin{cases} (d-n, d+n) & \text{if } n+d \text{ is odd} \\ (\frac{d-n}{2}, \frac{n+d}{2}) & \text{otherwise.} \end{cases}$$

We extend \mathcal{R} to Farey pairs by $\mathcal{R}(p, q) = (\mathcal{R}(q), \mathcal{R}(p))$ and then component-wise to Farey quadruples. Our next two lemmas verify that this is well-defined.

Lemma 3.5. *If (p, q) is a Farey pair, $\mathcal{R}(\mathcal{C}(p, q)) = \mathcal{C}(\mathcal{R}(p, q))$.*

Proof. This follows by a computation. \square

Finally, we show $\mathcal{R}(p)$ is a parent preserving bijection of the recursive tree \mathcal{T}_n .

Lemma 3.6. *The following holds for each word of length $n \geq 0$, $\mathbf{q}_{(w)} = (p_1, q_1, p_2, q_2) \in \mathcal{T}_n$.*

(1) *Rotations flip Type 2 and Type 3 children and preserve Type 1 children,*

$$\mathcal{R}(\mathbf{q}_{(w1)}) = \mathcal{R}(\mathbf{q}_{(w)})_1 \quad \mathcal{R}(\mathbf{q}_{(w2)}) = \mathcal{R}(\mathbf{q}_{(w)})_3 \quad \mathcal{R}(\mathbf{q}_{(w3)}) = \mathcal{R}(\mathbf{q}_{(w)})_2.$$

In particular,

$$\mathcal{R} \circ \mathcal{C}_1 = \mathcal{C}_1 \circ \mathcal{R} \quad \mathcal{R} \circ \mathcal{C}_2 = \mathcal{C}_3 \circ \mathcal{R} \quad \mathcal{R} \circ \mathcal{C}_3 = \mathcal{C}_2 \circ \mathcal{R}.$$

(2) *p_1 is the Farey child of (p_2, q_2) and $\mathcal{R}(q_1)$ is the Farey child of $\mathcal{R}(p_2, q_2)$*

(3) *The rotation preserves depth $\mathcal{R}(\mathcal{T}_n) = \mathcal{T}_n$.*

Proof. We prove the claims by induction on n , the depth of the tree; the base case $n = 0$ can be checked directly.

Proof of (1). Let

$$\mathbf{q}_{(w)} = (p'_1, q'_1, p'_2, q'_2)$$

so that

$$\begin{aligned}\mathbf{q}_{(w1)} &= (\mathcal{C}(p'_1, q'_1), p'_1, q'_1) \\ \mathbf{q}_{(w2)} &= (\mathcal{C}(p'_1, q'_2), p'_1, q'_2) \\ \mathbf{q}_{(w3)} &= (\mathcal{C}(p'_2, q'_1), p'_2, q'_1)\end{aligned}$$

By Lemma 3.5,

$$\begin{aligned}\mathcal{R}(\mathbf{q}_{(w)})_1 &= (\mathcal{C} \circ \mathcal{R}(p'_1, q'_1), \mathcal{R}(p'_1, q'_1)) \\ &= (\mathcal{R} \circ \mathcal{C}(p'_1, q'_1), \mathcal{R}(p'_1, q'_1)) \\ &= \mathcal{R}(\mathbf{q}_{(w1)}).\end{aligned}$$

For the other cases, we use the induction hypothesis together with the Lemma. Recall

$$\mathcal{R}(\mathbf{q}_{(w)}) = (\mathcal{R}(q_1), \mathcal{R}(p_1), \mathcal{R}(q_2), \mathcal{R}(p_2)),$$

hence

$$\begin{aligned}\mathcal{R}(\mathbf{q}_{(w)})_2 &= (\mathcal{C}(\mathcal{R}(q'_1), \mathcal{R}(p'_2)), \mathcal{R}(q'_1), \mathcal{R}(p'_2)) \\ &= (\mathcal{C} \circ \mathcal{R}(p'_2, q'_1), \mathcal{R}(p'_2, q'_1)) \\ &= (\mathcal{R} \circ \mathcal{C}(p'_2, q'_1), \mathcal{R}(p'_2, q'_1)) \\ &= \mathcal{R}(\mathbf{q}_{(w3)}).\end{aligned}$$

The other case is symmetric.

Proof of (2). By the inductive hypothesis (6), p_2, q_2 are vanilla Farey neighbors therefore p_1 is the vanilla Farey child by definition. Also, by (6) and (3) $\mathcal{R}(p_2, q_2)$ are also vanilla Farey neighbors. Moreover, by Lemma 3.4, $\mathcal{C} \circ \mathcal{R}(p_2, q_2) = \mathcal{R}(p_1, q_1) = \mathcal{R}(q_1), \mathcal{R}(p_1)$, meaning it is also a Farey child.

Proof of (3).

By the inductive hypothesis, $\mathcal{R}(T_{n-1}) = T_{n-1}$ and by definition, $T_n = \bigcup_{i=1}^3 \mathcal{C}_i \circ T_{n-1}$. Hence, by part (1) and the inductive hypothesis on (3),

$$\mathcal{R} \circ T_n = \bigcup_{i=1}^3 \mathcal{R} \circ \mathcal{C}_i \circ T_{n-1} = \bigcup_{i=1}^3 \mathcal{C}_i \circ \mathcal{R} \circ T_{n-1} = \bigcup_{i=1}^3 \mathcal{C}_i \circ T_{n-1} = T_n,$$

concluding the proof. □

In the subsequent sections we will show that the recursion on odometers and tiles also shares the same rotational symmetry.

4. ALMOST PSEUDO-SQUARE TILINGS

In this section we prove a technical tiling lemma which will allow us to show that the tiles which we define in the subsequent sections cover \mathbb{Z}^2 periodically.

We identify \mathbb{Z}^2 with $\mathbb{Z}[i]$. A *cell* is a unit square $s_x = \{x, x+1, x+i, x+1+i\} \subset \mathbb{Z}[i]$ and a *tile* is a simply connected union of cells whose boundary is a simple closed curve. The *vertices* of a tile are the Gaussian integers on its boundary. Let $(F_2, *)$ be the free group generated by $\{1, i\}$. For $w \in F_2$, let \hat{w} denote its involution, i.e., $\hat{w} * w = \{ \}$. Let $\mathbf{rev}(w)$

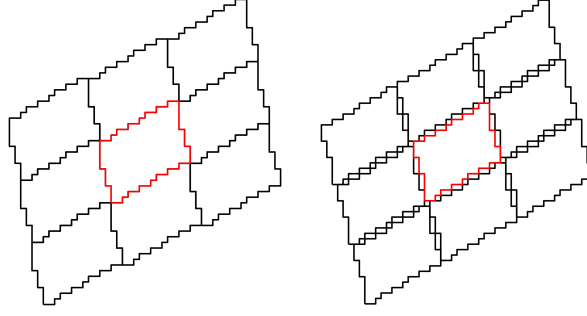


FIGURE 8. A surrounding of a pseudo-square tiling and an almost pseudo-square tiling as defined in Proposition 4.1 and Lemma 4.1 respectively.

denote the reversal of $w \in F_2$, $w[i]$ the i th letter of w , and $|w|$ the number of letters in w . The *boundary word* of a tile is a word $w \in F_2$ which represents a vertex walk around the boundary of the tile. In particular, $\sum w = 0$ and $\sum w' \neq 0$ for any non-empty subword w' of w , where \sum denotes the abelianization of F_2 .

A *tiling* of the plane is an infinite set of translations of a tile T where every cell is contained in exactly one copy of T . A tiling of T is (v_1, v_2) -*regular* if every tile T' in the tiling can be expressed as $T + kv_1 + k'v_2$ for $k, k' \in \mathbb{Z}$ and $v_1, v_2 \in \mathbb{Z}[i]$. That is, the translations of T by (v_1, v_2) generate the tiling.

Beauquier-Nivat [BN91] have a simple criteria for determining if a tile generates a regular tiling. Their criteria is expressed in terms of the boundary words of a tile, but can be interpreted geometrically as: a tile generates a regular tiling if it can be perfectly surrounded by copies of itself. We refer to a tiling satisfying the conditions in Proposition 4.1 as a *pseudo-square tiling*.

Proposition 4.1 ([BN91]). *If the boundary word of a tile, $w \in F_2$, can be expressed as*

$$w = w_1 * w_2 * \hat{w}_1 * \hat{w}_2,$$

then the tile generates a $(\sum w_1, \sum w_2)$ -regular tiling.

In our main argument, we require a technical modification of the notion of tiling in which bounded gaps are allowed. An *almost tiling*, \mathcal{T} , is an infinite set of translations of a tile T where every cell is contained in at most one tile and every $x \in \mathbb{Z}^2$ is a vertex of a cell in \mathcal{T} , i.e., there is $s_y \in \mathcal{T}$ with $x \in s_y$. The notion of regular with respect to a lattice is also extended to almost tilings.

We now give a sufficient condition for generating almost tilings. Roughly, this relaxation of tiling allows for slight gaps between cells in the surrounding of a tile. We will refer to the almost tiling from Lemma 4.1 as an *almost pseudo-square tiling*. See Figure 8 for an illustration of this.

Lemma 4.1. *Suppose $w = w_1 * w_2 * \widehat{\text{rev}(w_1)} * \widehat{\text{rev}(w_2)}$ is the boundary word of a tile T . Further suppose the following conditions on $w \in \{w_1, -i \cdot w_2\}$.*

- (1) *Monotonicity: $\{-1, -i\} \not\subset w$ and $w[1] = w[|w|] = 1$*

(2) Three cases on the form of w and its reversal:

(a) w is a palindrome, $w = \mathbf{rev}(w)$

(b) $w = (1 * 1 * i) * \tilde{w} * 1$, where \tilde{w} is a palindrome. Moreover, every i in w is followed by at least one 1.

(c) $w = 1 * \tilde{w} * (1 * 1 * 1)$ where \tilde{w} is a palindrome. Moreover, every i in w is followed by at least three 1s.

Then, T generates a $(\sum w_1 + i, \sum w_2 - 1)$ -regular almost tiling. Moreover, the only tiles in the tiling which share edges with T are $T \pm (\sum w_1 + i)$ and $T \pm (\sum w_2 - 1)$.

Proof. Let $(v_1, v_2) = (\sum w_1, \sum w_2)$. To show that T generates a $(v_1 + i, v_2 - 1)$ -regular almost tiling, by periodicity, it suffices to analyze one surrounding of T ,

$$S := \bigcup_{|k_1| \leq 1, |k_2| \leq 1} \{T + k_1(v_1 + i) + k_2(v_2 - 1)\},$$

see Figure 8. Specifically we show that the closure,

$$\bar{S} = \{s_x : x \in S \cap \mathbb{Z}^2\}.$$

is simply connected and no two cells in the decomposition of S overlap.

Observe that the boundary word of T implies it is 180-degree symmetric. Hence, S is 180-degree symmetric and we may reduce to analyzing the interfaces between T and its lower, right, and lower-right neighbors,

$$T_h := T + v_1 + i$$

$$T_v := T - v_2 + 1$$

$$T_d := T + v_1 - v_2 + 1 + i.$$

We show that the conditions imply no two pairs of edges cross and that every gap in the interface borders a cell of T .

Step 1: The bottom interface

We start with the bottom interface, T and T_v . Take the origin as the lower-left vertex of T so that cells along the bottom of T can be labelled by w_1 . By the definition and the translation offsets, vertices along the top edge of T_v can then be labeled by $\mathbf{rev}(w_1) + 1$. For $j \leq |w_1|$, let $x_j = \sum w_1[1 : j]$ and $y_j = 1 + \sum(\mathbf{rev}(w_1)[1 : j])$, where $w[1 : j]$ represents the first j letters of w . In particular, $x_0 = 0$ and $y_0 = 1$.

We now split the argument into three cases depending on the form of w_1 as dictated by (2).

Case (a): $w_1 = \mathbf{rev}(w_1)$

In this case, $y_j = 1 + \sum w_1[1 : j]$ and so

$$(22) \quad \text{Im}(x_j) = \text{Im}(y_j) \quad \text{and} \quad \text{Re}(x_j) = \text{Re}(y_j) - 1.$$

Therefore, any vertex y_j along the top edge of T_v is distance at most one from x_j , the lower left-corner of a cell in T .

To see that the top edge of T_v does not cross above the bottom edge of T , we use monotonicity. Suppose for sake of contradiction a crossing occurs. Since $w_1 = 1$, $x_1 = y_0$ and therefore there is a first j at which $y_j = x_{j+1}$ and $y_{j+1} = x_{j+2} + i$. Since $y_j = x_{j+1}$, by (22)

$$\text{Im}(y_j) = \text{Im}(x_{j+1}) = \text{Im}(y_{j+1}) \quad \text{and} \quad \text{Re}(y_j) = \text{Re}(x_{j+1}) = \text{Re}(y_{j+1}) - 1,$$

which implies by monotonicity that $y_{j+1} = y_j + 1$, a contradiction.

Case (b):

In this case

$$\begin{aligned} w_1 &= (1 * 1 * i) * \tilde{w} * 1 \\ \mathbf{rev}(w_1) &= 1 * \tilde{w} * (i * 1 * 1) \end{aligned}$$

Therefore, (after remembering the offset of T_v)

$$\begin{aligned} x_0 &= 0 & x_1 &= 1 & x_2 &= 2 & x_3 &= 2 + i \\ y_0 &= 1 & y_1 &= 2 & y_2 &= 2 + \tilde{w}[1] & y_3 &= 2 + \tilde{w}[1] + \tilde{w}[2]. \end{aligned}$$

also by the moreover clause, $y_2 = 3$ and

$$\begin{aligned} x_{3+|\tilde{w}|} &= (2 + i) + \sum \tilde{w} & x_{4+|\tilde{w}|} &= (3 + i) + \sum \tilde{w} \\ y_{1+|\tilde{w}|} &= (2) + \sum \tilde{w} & y_{2+|\tilde{w}|} &= (2 + i) + \sum \tilde{w} \\ y_{3+|\tilde{w}|} &= (3 + i) + \sum \tilde{w} & y_{4+|\tilde{w}|} &= (4 + i) + \sum \tilde{w} \end{aligned}$$

thus it suffices to consider $1 \leq j \leq 1 + |\tilde{w}|$ for which

$$(23) \quad x_{j+2} = y_j + i.$$

It remains to show this implies there are no crossings. Suppose for contradiction $y_j = x_{j'}$ and $y_{j+1} = y_j + i$ but $x_{j'+1} = x_{j'} + 1$. for some $1 \leq j \leq 1 + |\tilde{w}|$. By (24), $y_{j+1} = x_{j+2} = x_{j'} + i$. By monotonicity, $j' = j + 1$ and so $x_{j'+1} = x_{j'} + i$, a contradiction.

Case (c):

In this case,

$$\begin{aligned} w_1 &= 1 * \tilde{w} * (1 * 1 * 1) \\ \mathbf{rev}(w_1) &= (1 * 1 * 1) * \tilde{w} * 1 \end{aligned}$$

and so

$$\begin{aligned} x_0 &= 0 & x_1 &= 1 & x_2 &= 1 + \tilde{w}[1] \\ y_0 &= 1 & y_1 &= 2 & y_2 &= 3 & y_3 &= 4 \end{aligned}$$

and

$$\begin{aligned} x_{1+|\tilde{w}|} &= 1 + \sum \tilde{w} & x_{1+|\tilde{w}|+z} &= (1 + z) + \sum \tilde{w} & \text{for } z \leq 3 \\ y_{3+|\tilde{w}|} &= 4 + \sum \tilde{w} & y_{4+|\tilde{w}|} &= 5 + \sum \tilde{w}. \end{aligned}$$

We note that for all $2 \leq j \leq |\tilde{w}| + 3$,

$$(24) \quad y_j = x_{j-2} + 3.$$

Indeed, $x_{1+z} = 1 + \sum \tilde{w}[1 : z]$ and $y_{3+z} = 4 + \tilde{w}[1 : z]$ for $z \leq |\tilde{w}|$.

We claim that this together with the moreover clause implies no big gaps. Indeed, if $y_j = x_{j-2} + 3$, then $x_j = x_{j-2} + 1 + (1 \text{ or } i)$. In the first case, we are done. In the second case, $x_{j+2} = x_{j-2} + 1 + i + 2$.

(24) also implies no crossings. Indeed, suppose for contradiction $y_j = x_{j'}$ and $y_{j+1} = y_j + i$ but $x_{j'+1} = x_{j'} + 1$. for some $2 \leq j \leq 2 + |\tilde{w}|$. We have $y_j = x_{j-2} + 3$ and $y_{j+1} = x_{j-1} + 3$. This implies $x_{j-1} = x_{j-2} + i$ and hence the moreover clause implies $x_{j+2} = x_{j-1} + 3 =$

$x_{j-2} + 3 + i = y_j + i = y_{j+1}$. Monotonicity then implies $x_{j+1} = x_{j'} = y_j$, but this then contradicts $x_{j'+1} = x_{j'} + 1$.

Step 2: Conclude

After rotating, the arguments in Step 1 apply to the interface between T and T_h . We then check T and T_d . Let $z_0 = \sum w_1$ and note that the top left vertex of T_d is $z_0 + 1 + i$. By the assumption on the first and last letter of w_2 , the next vertices on the top and left edges of T_d are $z_0 + 2 + i$ and $z_0 + 1$ respectively while the next vertex on the right edge of T is $z_0 + i$. This implies that T does not overlap T_d and that the gap between the two tiles is of unit size.

Finally, by monotonicity, for any other pair of cells in S to overlap, there must first be a crossing on the horizontal or vertical edges which we have just shown to be impossible. \square

5. ZERO-ONE BOUNDARY STRINGS

In this section we start adding additional data to the hyperbola recursion, starting with a binary word recursion and then associate functions and tiles to the binary words.

5.1. A recursion on binary words. We associate to the each reduced fraction in the modified Farey recursion a binary word, and expose some basic properties. Specifically, given any initial Farey pair (p, q) we associate each descendant to a binary word, a word in the alphabet generated by the two letters, $\{p, q\} \in F_2$, by augmenting the recursion.

Given $w \in F_3$ and two binary words $p_t, q_t \in F_2$ we extend the child operator in (16) to pairs of binary words by

$$(25) \quad \mathcal{C}_{(w)}(p_t, q_t) = \begin{cases} (q_t q_t p_t, q_t p_t) & \text{if } \sum 1\{w_j = 1\} \text{ is even} \\ (p_t q_t q_t, p_t q_t) & \text{otherwise.} \end{cases}$$

Let $w_0 \in F_3$ describe (p, q) and $\mathbf{Q}_{(w_0)} = (\mathcal{C}_{w_0}(p, q), p, q)$ be the initial binary word quadruple in F_2 . Then, recursively, given $w \in F_3$ and $\mathbf{Q}_{(w)} = (p, q, p', q')$, each child Farey binary word quadruple is defined by

$$(26) \quad \begin{aligned} \mathbf{Q}_{(w*1)} &= (\mathcal{C}_{(w*1)}(p, q), p, q) \\ \mathbf{Q}_{(w*2)} &= (\mathcal{C}_{(w*2)}(p, q'), p, q') \\ \mathbf{Q}_{(w*3)} &= (\mathcal{C}_{(w*3)}(p', q), p', q). \end{aligned}$$

Recall that a palindrome $\tilde{w} \in F_2$ is a word that is equal to its reversal, $\tilde{w} = \mathbf{rev}(\tilde{w})$. An *almost palindrome* is a word $w = s_1 * \tilde{w} * s_2$, where $s_1, s_2 \in \{p, q\}$ are two letters and \tilde{w} is a palindrome. Write $w[1 : t]$ for the first t letters in w .

Lemma 5.1. *The following hold for every subsequent pair of binary words (p_t, q_t) produced by (26).*

- (1) *Both p_t and q_t are almost palindromes*
- (2) *If $\sum w_{0j}$ is even then all subsequent words begin with q and end with p and otherwise begin with p and end with q .*
- (3) *Let $n = \min(|p_t|, |q_t|)$ and $m = \min(|p_t|, 2|q_t|)$. Then,*

$$p_t[2 : n] = \mathbf{rev}(q_t)[2 : n] \quad p_t[2 : m] = \mathbf{rev}(q_t q_t)[2 : m].$$

Proof. We may suppose without loss of generality that $\sum 1\{w_{0_i} = 1\}$ is even as otherwise the subsequent statements follow by reversing.

Let $\mathbf{Q}_{(w)} = (p_{t+1}, q_{t+1}, p_t, q_t)$ be given and we will verify claims (1) and (2) for the child Farey pair and claim (3) for the parent Farey pair in the quadruple

$$\mathbf{Q}_{(w')} = (p_{t+2}, q_{t+2}, p'_{t+1}, q'_{t+1})$$

defined by (26). To do so, we must eliminate the degenerate cases $p'_{t+1} = p$ or $q'_{t+1} = q$. Fortunately, these can only occur if $w' = 3^k$ or $w' = 2^k$ for $k \geq 0$ respectively. An induction shows that

$$(27) \quad \begin{aligned} \mathbf{Q}_{(3^k)} &= (qp^k qp^{k+1}, qp^{k+1}, p, qp^k) \\ \mathbf{Q}_{(2^k)} &= (q^{2(k+1)}p, q^{2k+1}p, q^{2k}p, q), \end{aligned}$$

and we can verify the claim directly in these cases by inspection. We can then use (27) to also handle the cases $w' = 3^k\{1, 2\}$ or $w' = 2^k\{1, 3\}$.

Hence, we may assume none of $p_t, q_t, p_{t+1}, q_{t+1}$ are singletons, that is the induction hypotheses hold for each of them. We also suppose $\sum 1\{w_i = 1\}$ is even. By the induction hypotheses

$$p_t = qw^1p \quad q_t = qw^2p$$

for palindromes w^1 and w^2 and so

$$(28) \quad \begin{aligned} p_{t+1} &= qw^2pqw^2pqw^1p \\ q_{t+1} &= qw^2pqw^1p. \end{aligned}$$

Since p_{t+1} and q_{t+1} are almost palindromes and w^i are palindromes this implies the reversal relations

$$(29) \quad \begin{aligned} w^2pqw^1 &= w^1qpw^2 \\ w^2pqw^2pqw^1 &= w^1qpw^2qpw^2, \end{aligned}$$

since w^i are palindromes. We can use this to check claim (3). Using (29) and that w^i are palindromes,

$$\begin{aligned} \mathbf{rev}(q_{t+1}) &= pw^1qpw^2q \\ p_{t+1} &= qw^1qpw^2qpw^2p \\ \mathbf{rev}(q_{t+1}q_{t+1}) &= pw^1qpw^2qpw^2pqw^1q, \end{aligned}$$

For claim (2), the possible decompositions of (p_{t+2}, q_{t+2}) are

$$\begin{aligned} (p_{t+1}q_{t+1}q_{t+1}, p_{t+1}q_{t+1}) &\quad \text{Type 1} \\ (q_tq_t p_{t+1}, q_t p_{t+1}) &\quad \text{Type 2} \\ (q_{t+1}q_{t+1}p_t, q_{t+1}p_t) &\quad \text{Type 3.} \end{aligned}$$

The reversal(29) relations together (28) show that each of the decompositions are almost palindromes. We show only the odd Type 1 case as the rest are similar. First, write using (28)

$$p_{t+1}q_{t+1}q_{t+1} = qw^2pqw^2pqw^1pqw^2pqw^1pqw^2pqw^1p,$$

and then use (29) to check

$$\begin{aligned}
 \mathbf{rev}(w^2pqw^2pqw^1pqw^2pqw^1pqw^2pqw^1) &= [w^1qp w^2]qp[w^1qp w^2]qp[w^1qp w^2qp w^2] \\
 &= [w^2pq(w^1)]qp[w^2]pq(w^1qp[w^2])pqw^2pqw^1 \\
 &= w^2pq(w^2pqw^1)pq(w^2pqw^1)pqw^2pqw^1.
 \end{aligned}$$

□

A word $w \in F_2$ is *proper* if it is an almost palindrome that begins and ends with different letters.

5.2. Basic definitions. We next associate tile and function data to the binary word recursion. But in order to do so, we must recall and modify some definitions from [LPS16]. A *tile* T is now a finite subset of \mathbb{Z}^2 . Let $c(T)$ denote the coordinate-wise minimum T , (geometrically the lower-left vertex). A *partial odometer* is a function $h : T \rightarrow \mathbb{Z}$. The domain of h is $T(h)$ and $s(h) \in \mathbb{C}$ is the *slope* of T , the average of

$$\begin{aligned}
 (30) \quad & \frac{1}{2} (h(x+1) - h(x) + h(x+1+\mathbf{i}) - h(x+\mathbf{i})) + \\
 & \frac{\mathbf{i}}{2} (h(x+\mathbf{i}) - h(x) + h(x+1+\mathbf{i}) - h(x+1))
 \end{aligned}$$

for $x \in T$. Two partial odometers o_1 and o_2 are *translations* of one another if

$$(31) \quad T(o_1) = T(o_2) + v \quad \text{and} \quad o_1(x) = o_2(x+v) + a \cdot x + b$$

for some $v, a \in \mathbb{Z}^2$ and $b \in \mathbb{Z}$.

Partial odometers o_1 and o_2 are *compatible* if $o_1 - o_2 = c$ on $T(o_1) \cap T(o_2)$ for some *offset constant* $c \in \mathbb{Z}$. As in [LPS16], if the offset constant is 0 or the tiles do not overlap then $o_1 \cup o_2$ is the common extension to $T(o_1) \cup T(o_2)$. We recall for later reference the following lemma which will allow us to construct global odometers from pairwise compatible partial odometers.

Lemma 5.2 (Lemma 9.2 in [LPS16]). *If $\mathcal{S} = \{o_i\}$ is a collection of pairwise compatible partial odometers such that $\{T(o_i)\}$ forms an almost pseudo-square tiling then there is a function $g : \mathbb{Z}^2 \rightarrow \mathbb{Z}$ unique up to adding a constant that is compatible with every $o_i \in \mathcal{S}$.*

5.3. Even-odd boundary strings. We now associate additional data to each binary word constructed in the first subsection. The result in this subsection will form a key tool in verifying correctness of the subsequent tile and odometer recursion.

We first adapt the notion of *boundary string* from [LPS16] to our setting. Suppose T_p and T_q are tiles which generate $(v_{p,1}, v_{p,2})$ and $(v_{q,1}, v_{q,2})$ regular almost pseudo-square tilings respectively. A q - p *boundary string* is a collection of tiles $T_i \in \{T_q, T_p\}$ such that

$$(32) \quad c(T_i) - c(T_{i-1}) = \begin{cases} v_{p,j} & \text{if } T_{i-1} = T_p \\ v_{q,j} & \text{if } T_{i-1} = T_q, \end{cases}$$

for fixed $j \in \{1, 2\}$. A q - p reversed boundary-string is also a collection of tiles $T_i \in \{T_q, T_p\}$ but with different offsets:

$$(33) \quad c(T_i) - c(T_{i-1}) = \begin{cases} v_{p,j} + (v_{p,j'} - v_{q,j'}) & \text{if } pq \\ v_{p,j} & \text{if } pp \\ v_{q,j} + (v_{q,j'} - v_{p,j'}) & \text{if } qp \\ v_{q,j} & \text{if } qq, \end{cases}$$

where $(j, j') \in \{(1, 2), (2, 1)\}$ is fixed and the right column denotes the tile tuple, *e.g.*, the first row is $(T_{i-1}, T_i) = (T_p, T_q)$. When $j = 1$, a boundary string is *horizontal* and otherwise is *vertical*. We label a boundary string by a binary word $w \in F_2$, \mathcal{B}_w where a superscript r indicates it is reversed.

A horizontal or vertical *stacked boundary string* for $w \in F_2$ is a union of $\{T_i^+\} := \mathcal{B}_w$ and $\{T_i^-\} := \mathcal{B}_{\text{rev}(w)}^r$ both oriented in the same direction. The first tiles T_1^+ and T_1^- in each string and the shared direction dictate the relative positions,

$$(34) \quad c(T_1^+) - c(T_1^-) = v_{n/d', j'}$$

where $j' \in \{1, 2\}$ is the perpendicular direction and $n/d' \in \{p, q\}$ is the type of T_1^- . See Figure 9.

We now observe that tile offsets between perpendicular adjacent tiles in a stacked boundary string are given by a simple formula if the binary word describing the string is an almost palindrome.

Lemma 5.3. *If w is an almost palindrome, then for all $1 < i \leq |w|$*

$$c(T_i^+) - c(T_i^-) = v_{n/d', j'} + (v_{a,j} - v_{b,j})$$

where $j' \in \{1, 2\}$ is the perpendicular direction, $n/d', a, b \in \{p, q\}$ is the type of T_i^- , T_1^+ and T_1^- respectively.

Proof. For concreteness and since w is an almost palindrome, take $j = 1$, $T_1^+ = T_p$ and $T_1^- = T_q$. If T_2^- and T_2^+ are both of type p , then

$$\begin{aligned} c(T_2^+) - c(T_2^-) &= (c(T_2^+) - c(T_1^+)) + (c(T_1^+) - c(T_1^-)) + (c(T_1^-) - c(T_2^-)) \\ &= v_{p,1} + v_{q,2} - (v_{q,1} + (v_{q,2} - v_{p,2})) \\ &= v_{p,2} + (v_{p,1} - v_{q,1}). \end{aligned}$$

If T_2^- and T_2^+ are both of type q , then

$$c(T_2^+) - c(T_2^-) = v_{p,1} + v_{q,2} - v_{q,1}.$$

Conclude by similar computations together with an induction on $1 < i \leq |w|$. □

5.4. A degenerate boundary string. We now examine a degenerate boundary string which we will show completely describes the recursion. Due to the degenerate nature of the tiles in the string, the offsets in the definition of boundary string must be modified slightly. Let $p, q = 0/1, 1/1$ and v_* be as defined in Section 3:

$$\begin{aligned} v_{p,1} &= 2 & v_{p,2} &= -1 + i \\ v_{q,1} &= 1 + i & v_{q,2} &= 2i. \end{aligned}$$

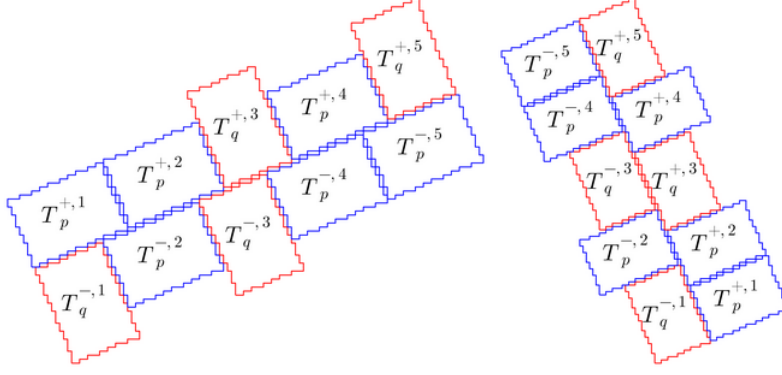


FIGURE 9. Stacked horizontal and vertical boundary strings. The superscripts $+$, $-$ denote the non-reversed and reversed strings respectively. Here the strings are outlined in the dual lattice.

(Note that we do include the factor of 2 here.)

The *zero-tile* is $T_0 = \{0, i, 2i, 1, 1 + i, 1 + 2i\}$ and the *one-tile* is $T_1 = \{0, i, 1, 1 + i\}$. A *zero-one horizontal* boundary string is a collection of tiles $T_i \in \{T_0, T_1\}$ with offsets given by

$$(35) \quad c(T_i) - c(T_{i-1}) = \begin{cases} v_{q,1} & \text{if } T_i = T_q \\ v_{p,1} & \text{if } T_i = T_p, \end{cases}$$

and in the reversed case

$$(36) \quad c(T_i) - c(T_{i-1}) = \begin{cases} v_{q,1} + 1 & \text{if } pq \\ v_{p,1} & \text{if } pp \\ v_{p,1} - 1 & \text{if } qp \\ v_{q,1} & \text{if } qq. \end{cases}$$

We further impose that every (reversed) horizontal zero-one boundary string begins with T_1 (T_0).

A *zero-one stacked horizontal* boundary string is a union of a horizontal zero-one boundary string and its reversal where

$$(37) \quad c(T^{+,1}) - c(T^{-,1}) = v_{p,2} + i.$$

Unfortunately, in this case the stacked boundary strings may leave gaps which are too large. This occurs for exactly one particular interface, qq , which we have displayed in Figure 10. To fix this, we fill the gap by requiring that whenever T_1 follows a T_1 , the subsequent tile is replaced by an enlarged version:

$$(38) \quad T_1^d = T_1 \cup \{i - 1, 1 - i\},$$

but there are no other changes, *i.e.*, we take $c(T_1^d) = c(T_1) = 0$.

To define vertical strings, we simply rotate each of the above conditions by 90 degrees but exclude the doubled tiles. To be specific, a *zero-one vertical* boundary string is also a collection of tiles $T_i \in \{T_0, T_1\}$ but with rotated offsets:

$$(39) \quad c(T_i) - c(T_{i-1}) = \begin{cases} v_{q,2} & \text{if } T_i = T_q \\ v_{p,2} & \text{if } T_i = T_p \end{cases}$$



FIGURE 10. A gap between a zero-one horizontal stacked boundary string corresponding to the word $qqqp$. Here we are outlining tiles on a square grid where each $x \in \mathbb{Z}[i]$ is in the center of a square. On the left, points in the stacked string are filled in with either black (T_0) or yellow (T_1). On the right the outlines and annotations are displayed; the superscripts $+$, $-$ denote the non-reversed and reversed strings respectively.

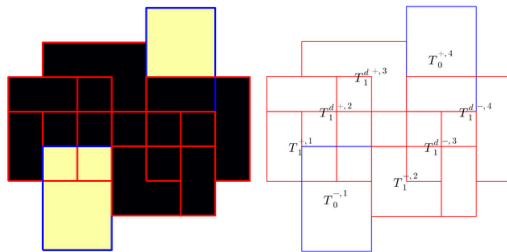


FIGURE 11. As Figure 10 but with gap fixed by T_1^d .

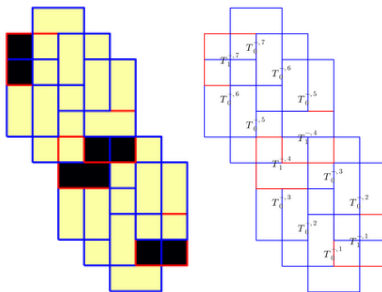


FIGURE 12. A vertical stacked zero-one boundary string with the same labeling scheme as Figure 10.

and in the reversed case

$$(40) \quad c(T_i) - c(T_{i-1}) = \begin{cases} v_{p,2} + i & \text{if } pq \\ v_{p,2} & \text{if } pp \\ v_{q,2} - i & \text{if } qp \\ v_{q,2} & \text{if } qq. \end{cases}$$

A *zero-one stacked vertical* boundary string is a union of a vertical even-odd boundary string and its reversal where

$$(41) \quad c(T^{+,1}) - c(T^{-,1}) = -v_{q,1}.$$

In the vertical case, we do not use doubled tiles and we further impose that every (reversed) vertical zero-one boundary string begins with T_0 (T_1). See an example of a stacked vertical zero-one boundary string in Figure 12. In both horizontal and vertical cases we label boundary strings by binary words in F_2 and we also label stacked boundary strings by the non-reversed word.

We observe a similar counterpart to Lemma 5.3.

Lemma 5.4. *If w is an almost palindrome beginning with q and ending with p then the offsets between perpendicular tiles in the stacked string are fixed: in the horizontal case*

$$\begin{aligned} c(T_1^{+,1}) - c(T_1^{-,1}) &= -1 + 2i = v_{p,2} + i & qp \\ c(T_1^+) - c(T_1^-) &= 2i - 2 = v_{p,2} + i - 1 & qq \\ c(T_0^+) - c(T_0^-) &= 2i - 1 = v_{p,2} + i & pp \\ c(T_{|w|}^+) - c(T_{|w|}^-) &= 1 - i = (v_{p,1} - v_{q,1}) + (v_{p,2} + i - 1) & pq \end{aligned}$$

and in the vertical case

$$\begin{aligned} c(T_1^{+,1}) - c(T_1^{-,1}) &= -(i + 1) = -v_{q,1} & pq \\ c(T_1^+) - c(T_1^-) &= -(i + 1) = -v_{q,1} & qq \\ c(T_0^+) - c(T_0^-) &= -(2 + i) = v_{p,2} - v_{q,2} + i - v_{q,1} & pp \\ c(T_{|w|}^+) - c(T_{|w|}^-) &= -1 = -v_{q,1} + i & qp, \end{aligned}$$

□

In particular, the intersections of boundary strings reduces to a finite check which is displayed in Figures 13 and 14 respectively. We use this in the next section to assert compatibility of function data on boundary strings .

5.5. Function data. We now associate function data to zero-one boundary strings. Lemma 5.4 will be a key tool in proving pairwise compatibility. Recall the affine offsets associated to the hyperbola bases,

$$\begin{aligned} a_{p,1} &= 0 & a_{p,2} &= -i \\ a_{q,1} &= 0 & a_{q,2} &= 1 - i, \end{aligned}$$

for $p, q = 0//1, 1//1$.

The *zero-odometer* is any translation of $o_0 : T_0 \rightarrow \mathbb{Z}$, defined by $o_0(0) = o_0(1) = o_0(i) = o_0(1 + i) = 0$ and $o_0(2i) = o_0(1 + 2i) = -1$. The *one-odometer* is any translation of $o_1 : T_1 \rightarrow \mathbb{Z}$, defined by $o_1(0) = o_1(1) = o_1(1 + i) = 0$ and $o_1(i) = -1$. The *enlarged one-odometer* is any translation of $o_1^d : T_1^d \rightarrow \mathbb{Z}$ defined by $o_1^d = o_1$ on T_1 and $o_1^d(i - 1) = -2$, $o_1^d(1 - i) = 0$.

A sequence of zero/one-odometers $\{o_i\}$ *respects* a zero-one boundary string $\{T_i\}$ if each successive tile T_i is the domain of o_i and

$$(42) \quad \begin{aligned} s(o_{i+1}) - s(o_i) &= a_{i,j} & \text{not reversed case} \\ s(o_{i+1}) - s(o_i) &= a_{i,j} + (a_{i,j'} - a_{i+1,j'}) & \text{reversed case,} \end{aligned}$$

where $(j, j') \in \{1, 2\}$ are the direction and perpendicular direction respectively.

From Figure 13, one can see some consecutive pairs of tiles do not overlap. This means odometers corresponding to such tiles may blow up across the boundary. We fix this by

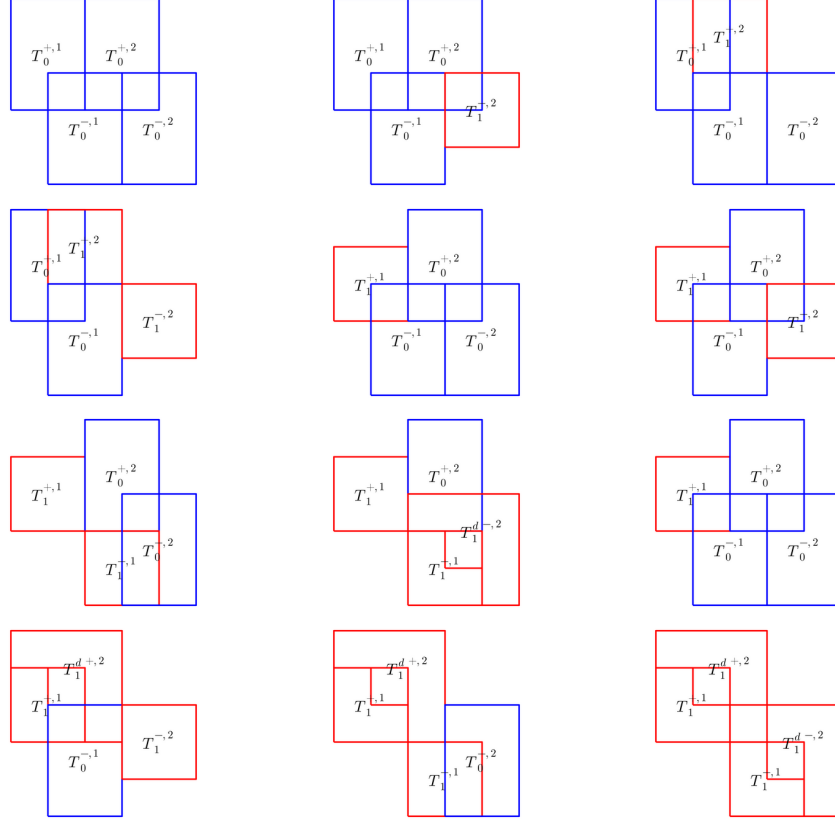


FIGURE 13. Twelve possible overlaps in a stacked zero-one horizontal boundary string with labeling as Figure 10.

requiring a further compatibility relation between pairs of non-overlapping tiles. We assume that if T_1, T_2 are a consecutive sequence of horizontal tiles that do not overlap then, after a shared translation o_i and o_{i+1} are constant across the shared boundary. That is, after the translation, $o_i(x) = o_{i+1}(y)$ for all $|y - x| = 1$. In the vertical case, if T_i and T_{i+1} do not overlap, then they must both be type 1/1; we assume that after a shared translation, $o_{i+1}(y) - o_i(x) = -1$ for $|y - x| = 1$.

We now check existence, using Lemma 5.4.

Lemma 5.5. *Given any word w , a sequence of zero/one odometers which respects its boundary string or its reversal exists. Moreover, if w is an almost palindrome, then there exists a sequence of odometers $\{o_i^+\}$, and $\{o_i^-\}$ respecting $\mathcal{B}_w = \{T_i^+\}$ and a sequence $\{o_i^-\}$ respecting the reversed string $\mathcal{B}_{\text{rev}(w)}^r$ living in the stacked string where $s(o_1^+) - s(o_1^-) = 0$ in the vertical case and $s(o_1^+) - s(o_1^-) = a_{p,2}$ in the horizontal case.*

Proof. From the definitions, one can see that no three consecutive pairs of tiles in a boundary string can overlap - only two consecutive pairs can. Therefore, existence of a sequence of zero/one odometers respecting a boundary string reduces to checking pairwise compatibility between partial odometers for consecutive tiles. Since compatibility is an affine invariant relationship, we can translate so that the first odometer is exactly o_1 or o_0 . This then reduces the compatibility check to a finite one.

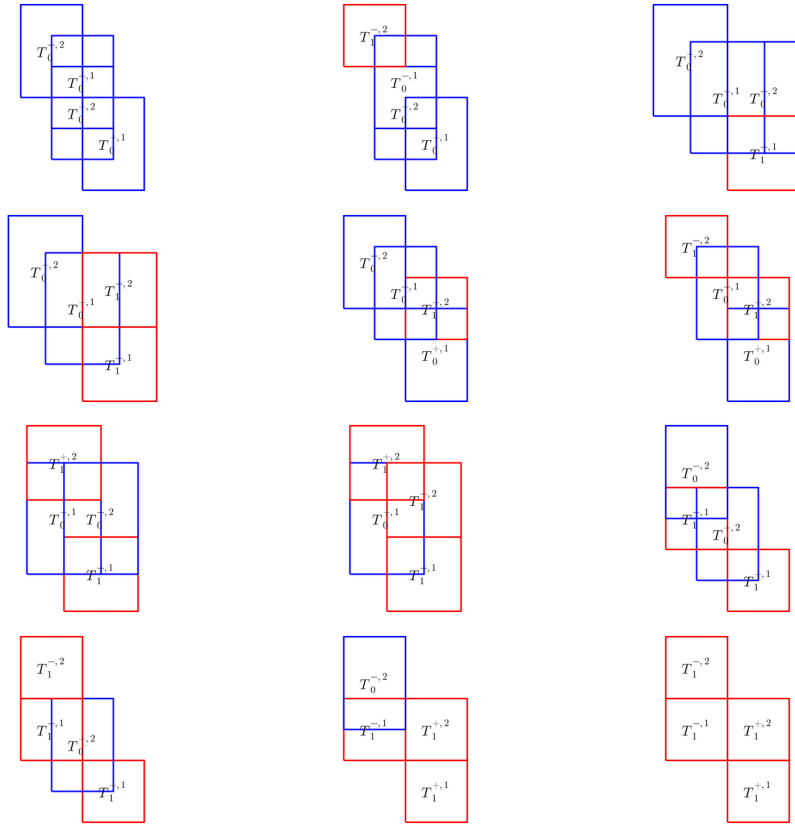


FIGURE 14. Twelve possible overlaps in a stacked zero-one vertical boundary string with labeling as Figure 10.

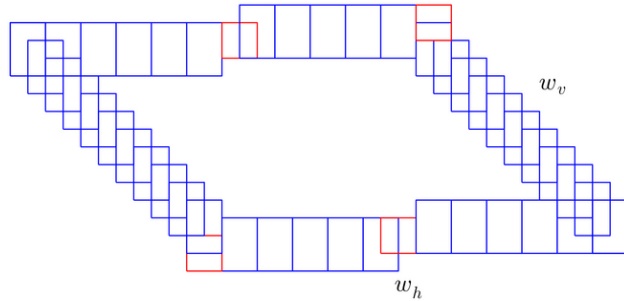


FIGURE 15. The boundary of a (w_h, w_v) -pseudo-square tile where w_h is the horizontal word qp^kqp^{k+1} and w_v is the vertical word $p^{2k+1}q$ for $k = 5$.

The existence problem for a stacked string is similar - by Lemma 5.4, there are only twelve possible cases for overlaps between tiles in a stacked string. We have enumerated these cases in Figures 13 and 14. □

5.6. Pseudo-square tiles and boundary strings. We now associate horizontal and vertical boundary strings to tiles and partial odometers. Let (w_h, w_v) denote almost palindromes which define zero-one horizontal and vertical boundary strings respectively.

Definition 1. A (w_h, w_v) -pseudo-square is a tile, T , which can be decomposed along its boundary into a sequence of subtiles

$$\mathcal{T}_{h,v} := \{T_{i,h}^+\} \cup \{T_{i,h}^-\} \cup \{T_{i,v}^+\} \cup \{T_{i,v}^-\}$$

each of which respectively form a w_h , $\mathbf{rev}(w_h)$, w_v , and $\mathbf{rev}(w_v)$ zero-one horizontal, reversed horizontal, vertical, and reversed vertical boundary string. That is, $\mathcal{T}_{h,v} \subset T$, $c(T_{1,h}^+) = c(T_{1,v}^-) = c(T)$ and $\partial T \cap \mathcal{T}_{h,v} = \partial T$.

A partial odometer $o : T \rightarrow \mathbb{Z}$ respects (w_h, w_v) if its restrictions to $\mathcal{T}_{h,v}$ respect w_h -horizontal, w_v -vertical, and $\mathbf{rev}(w_h)$ -reversed-horizontal and $\mathbf{rev}(w_v)$ -reversed-vertical zero-one boundary strings respectively.

We sometimes will overload notation and refer to the word describing the boundary string as the set of tiles.

We now extend the rotation operator to such pseudo-squares. For a binary word w , let $\mathcal{F}(w)$ denote the flipping operator which flips every p to a q and vice versa. Then,

$$(43) \quad \mathcal{R}(w_h, w_v) = (\mathcal{F}(w_v), \mathcal{F}(w_h))$$

sends a pair of proper almost horizontal/vertical strings to a rotated pair.

Lemma 5.6. *Every such tile is 180-degree symmetric and the rotation operator rotates the tile by 90 degrees and sends each rotated boundary strings to exactly the corresponding specified boundary string.*

We also require the notion of a tile odometer respecting only a horizontal boundary or vertical boundary string.

Definition 2. A $w_{h/v}$ -pseudo-square is a tile, T , whose boundary contains (but may not be equal to)

$$\mathcal{T}_{h,*} = \{T_{i,h}^+\} \cup \{T_{i,h}^-\}$$

or

$$\mathcal{T}_{*,v} = \{T_{i,v}^+\} \cup \{T_{i,v}^-\},$$

where T are as in Definition 1 and either $c(T) = c(T_{1,h}^+)$ or $c(T) = c(T_{1,v}^-)$

A partial odometer $o : T \rightarrow \mathbb{Z}$ respects $w_{h/v}$ if its restriction to $\mathcal{T}_{h,*}$ are w_h -horizontal and $\mathbf{rev}(w_h)$ -reversed-horizontal strings or its restriction to $\mathcal{T}_{*,v}$ are w_v and $\mathbf{rev}(w_v)$ -reversed-vertical zero-one boundary strings respectively.

5.7. Explicit formulas for zero-one boundary strings. We collect in this section some explicit formulas for zero-one boundary strings. In particular, these will correspond to the degenerate base cases in (27).

5.7.1. Horizontal boundary strings. We note the form of the odometers after a translation. The zero-odometer translated by $-a_{p,2}$, $\hat{o}_0 : T_0 \rightarrow \mathbb{Z}$ is given by $o_0(0) = o_0(1) = -1$ and $o_0(i) = o_0(1+i) = 0 = o_0(2i) = o_0(1+2i) = 0$. The one-odometer translated by $-a_{q,2}$, $\hat{o}_q : T_1 \rightarrow \mathbb{Z}$ is given by $\hat{o}_q(0) = \hat{o}_q(i) = \hat{o}_q(1+i)$ and $\hat{o}_q(1) = -1$. Similarly, the enlarged one-odometer translated by $-a_{q,2}$, $\hat{o}^d : T_1^d \rightarrow \mathbb{Z}$ is given by $\hat{o}^d = \hat{o}$ on T_1 and $\hat{o}(1-i) = -2$, $\hat{o}(i-1) = 0$.

Lemma 5.7. *Let $\{o_i\}$ respect $\{T_i\}$, a horizontal boundary string. If $o_1 = o_{0/1}$ or $o_1 = o_{1/1}$ on T_1 , then each subsequent odometer o_i matches either $o_{1/1}$ or $o_{0/1}$ exactly.*

Similarly, if $\{\hat{o}_i\}$ respects a reversed horizontal boundary string and $\hat{o}_1 = \hat{o}_{0/1}$ or $\hat{o}_1 = \hat{o}_{1/1}$, then all subsequent odometers match the base odometers exactly

Proof. This is immediate from the construction above. \square

5.7.2. Vertical boundary strings. The vertical boundary string case is more involved due to the fact that the vertical shifts involve affine factors. Fix $k \geq 1$. The following functions, corresponding to the affine growth of the hyperbola bases appear, depending on which vertical string is used:

$$(44) \quad T(j) = -j(j+1)/2 \quad Q(j) = \lfloor \frac{j^2}{4} \rfloor$$

Case 1: $p^k q$ and its reversal. Suppose $o_1^+ = o_{0/1}$ on T_1 . Then, for $1 \leq j \leq k$

$$o_j^+ = \begin{bmatrix} T(j) & T(j) \\ T(j-1) & T(j-1) \\ T(j-2) & T(j-2) \end{bmatrix}$$

and

$$o_{k+1}^+ = \begin{bmatrix} T(k+1) & T(k+1)+1 \\ T(k) & T(k) \end{bmatrix}$$

If $o_1^- = o_{0/1}$ on $T_{0/1}$ then similarly, the reversed word must be

$$o_j^- = \begin{bmatrix} T(j+1)+2 & T(j+1)+3 \\ T(j)+1 & T(j)+2 \\ T(j-1) & T(j-1)+1 \end{bmatrix}$$

for $2 \leq j \leq k+1$.

Case 2: pq^k and its reversal. If $o_1^+ = o_{0/1}$ on $T_{0/1}$ then for $2 \leq j \leq k+1$

$$o_j^+ = \begin{bmatrix} Q(j'+2)+1 & Q(j'+1) \\ Q(j'+1)+1 & Q(j') \end{bmatrix}$$

on T_j where $j' = 2(j-1)$.

Similarly, in the reversed case, if $o_1^- = o_{1/1}$ on $T_{1/1}$ then for $1 \leq j \leq k$

$$o_j^- = \begin{bmatrix} Q(2j) & Q(2j-1) \\ Q(2j-1) & Q(2j-2) \end{bmatrix}$$

and

$$o_{k+1}^- = \begin{bmatrix} Q(2k+2) & Q(2k+1)-1 \\ Q(2k+1) & Q(2k) \\ Q(2k) & Q(2k-1) \end{bmatrix}$$

Case 3: $pq^k pq^{k+1}$. If $o_1^+ = o_{0/1}$ on $T_{0/1}$, then the first $(k+1)$ tile odometers must be as Case 2 above. Then

$$o_{k+2} = \begin{bmatrix} Q(2(k+1)+3)+3 & Q(2(k+1)+2)+1 \\ Q(2(k+1)+2)+3 & Q(2(k+1)+1)+1 \\ Q(2(k+1)+1) & Q(2(k+1))+1 \end{bmatrix}$$

on $T_{k+2} = T_{0/1} + v$ (some affine shift). Then, for $k+3 \leq j \leq 2k+3$

$$o_j = \begin{bmatrix} Q(j''+4)+3 & Q(j''+3)+1 \\ Q(j''+3)+3 & Q(j''+2)+1 \end{bmatrix}$$

for $j'' = 2(j-2)$.

Similarly in the reversed case if $o_1^- = o_{1/1}$ on $T_{1/1}$ then the first $(k+2)$ tiles must be as Case 2 above. Then, for $(k+3) \leq j \leq 2k+2$,

$$o_j^- = \begin{bmatrix} Q(2(j-1)+2)+1 & Q(2(j-1)+1) \\ Q(2(j-1)+1)+1 & Q(2(j-1)) \end{bmatrix}$$

and

$$o_{2k+3}^- = \begin{bmatrix} Q(2w+2)+1 & Q(2w+1) \\ Q(2w+1)+1 & Q(2w) \\ Q(2w)+1 & Q(2w-1) \end{bmatrix}$$

for $w = 2(k+1)$.

Proof. These are verified by induction and the definition of the affine offsets. \square

6. BASE CASES

Before we extend the hyperbola recursion to all odometers and tiles, we study a degenerate family and in fact prove Theorem 1.3 for this family. The reader is encouraged to skim or skip this section and come back to it after reading the general recursive algorithm in the next section

The reduced fractions which we analyze here are those in a Farey quadruple where at least one of the two parents is $(0/1)$ or $(1/1)$. Specifically, we prove the following.

Proposition 6.1. *For each Farey quadruple of the form $\mathbf{q}_{(w)} = (p_1, q_1, p_2, q_2)$ where $w = 3^k$ or 2^k for $k \geq 0$ there is a quadruple of standard and alternate tile odometers*

$$(o_{p_1}, o_{q_1}, o_{p_2}, o_{q_2}) \quad \text{and} \quad (\hat{o}_{p_1}, \hat{o}_{q_1}, \hat{o}_{p_2}, \hat{o}_{q_2})$$

with finite domains, $T(o_{n/d}) = T_{n/d}$ and $T(\hat{o}_{n/d}) = \hat{T}_{n/d}$. The tile odometers of each such child Farey pair satisfy the following properties.

- (a) Under the lattice $L'(n/d)$, $T(n/d)$ generates an almost pseudo-square tiling
- (b) $\hat{T}(n/d)$ covers \mathbb{Z}^2 under $L'(n/d)$
- (c) There exist unique, distinct recurrent extensions $o_{n/d} : \mathbb{Z}^2 \rightarrow \mathbb{Z}$ and $\hat{o}_{n/d} : \mathbb{Z}^2 \rightarrow \mathbb{Z}$ satisfying the correct growth dictated by 9.
- (d) $T(n/d)$ is a (w_h, w_v) -pseudo-square which $o_{n/d}$ respects:

Standard case		w_h	w_v
3^k odd, $k \geq 1$	$1/d, d \geq 4$ even	$qp^k qp^{k+1}$	$p^{2k+1}q$
3^k even, $k \geq 0$	$1/d, d \geq 3$ even	qp^{k+1}	$p^{2(k+1)}q$
2^k odd, $k \geq 0$	$\mathcal{R}(1/d) d \geq 3$ even	$q^{2(k+1)}p$	pq^{k+1}
2^k even, $k \geq 1$	$\mathcal{R}(1/d), d \geq 4$ even	$q^{2k+1}p$	$pq^k pq^{k+1}$

The first column denotes a word which selects a degenerate Farey quadruple and the parity of the reduced fraction displayed in the second column.

(e) $\hat{T}(n/d)$ is a $w_{h/v}$ -pseudo-square which $\hat{o}_{n/d}$ respects:

Alternate case		w_h	w_v
3^k odd, $k \geq 1$	$1/d, d \geq 4$ even	-	$p^{2k+1}q$
3^k even, $k \geq 0$	$1/d, d \geq 3$ even	qp^{k+1}	-
2^k odd, $k \geq 0$	$\mathcal{R}(1/d) d \geq 3$ even	-	pq^{k+1}
2^k even, $k \geq 1$	$\mathcal{R}(1/d), d \geq 4$ even	$q^{2k+1}p$	-

In particular, the alternates coincide with the standards on one set of parallel boundaries.

(f) Some later odometers contain exact translations of earlier odometers. To state this succinctly, write $w(p, q)$ for the even and odd reduced fraction in the child Farey pair of $\mathbf{q}_{(w)}$ and let $T(n/d)(v) = T(n/d) \cup (T(n/d) + v)$ for $v \in \mathbb{Z}[i]$ and $n/d \in \{p, q\}$. The following holds for all $k \geq 1$:

$$\begin{aligned}
 (45) \quad & T(3^k(p)) \supset T(q, v_{q,1} + v_{p,1} + v_{p,2}) & \text{offset} = 0 \\
 & \hat{T}(3^k(p)) \supset T(q, v_{q,1} + v_{p,1} + 2v_{p,2}) & \text{offset} = 0 \\
 & \hat{T}(3^k(q)) \supset T(q, -v_{q,1} - v_{p,1}) & \text{offset} = v_{p,2} + v_{p,1}
 \end{aligned}$$

where $(p, q) = 3^{k-1}(p, q)$ and

$$\begin{aligned}
 (46) \quad & T(2^k(q)) \supset T(p, v_{p,2} + v_{q,2} - v_{q,1}) & \text{offset} = v_{q,1} \\
 & \hat{T}(2^k(q)) \supset T(p, v_{p,2} + v_{q,2} - 2v_{q,1}) & \text{offset} = v_{q,1} \\
 & \hat{T}(2^k(p)) \supset T(p, v_{p,2} + v_{q,2}) & \text{offset} = v_{q,1}
 \end{aligned}$$

where $(p, q) = 2^{k-1}(p, q)$. The offset column records $c(T_1) - c(T_2)$ where T_1 is the tile in the second column and T_2 is the tile in the first column.

The tile odometers for $k \geq 1$ have an analagous decomposition with affine factors and translations dictated by (45) and (46). For example, the restriction of $o_{3^k(p)}$ to $T(q, v_{q,1} + v_{p,1} + v_{p,2})$ is exactly equal to translated earlier tile odometers, $o_q^1 \cup o_q^2$ where $c(T(o_q^1) - c(T_{o_{3^k(p)}})) = 0$, $T(o_q^1) \cup T(o_q^2) = T(q, v_{q,1} + v_{p,1} + v_{p,2})$, $s(o_q^1) - s(o_q^2) = a_{p,2}$, and $s(o_q^2) - s(o_{3^k(p)}) = 0$.

(g) Some later odometers contain partial translations of earlier odometers. The following holds for all $k \geq 1$ (using the same notation as the previous item):

$$(47) \quad T(3^k(q)) \supset T(q, v_{p,1} + 2v_{p,2}) \quad \text{offset} = 0$$

where $(p, q) = 3^{k-1}(p, q)$ and

$$(48) \quad T(2^k(p)) \supset T(p, -2v_{q,1} + v_{q,2}) \quad \text{offset} = 2v_{q,1}$$

where $(p, q) = 2^{k-1}(p, q)$. The tile odometers for $k \geq 1$ have an analogous decomposition (as in the previous item) but only after removing two corner cells from each of the subtiles on the right-hand-side:

$$(49) \quad T^{sm}(q) = T(q) \setminus \{c_1 \cup c_2\} \quad \text{where } (p, q) = 3^{k-1}(p, q)$$

where $c_1 = c(T(q))$ and $c_2 = c_1 + (v_{q,1} + v_{q,2} - v_{p,2})$ and

$$(50) \quad T^{sm}(p) = T(p) \setminus \{c'_1 \cup c'_2\} \quad \text{where } (p, q) = 2^{k-1}(p, q)$$

where $c'_1 = c(T(p)) + v_{p,1} - i$ and $c'_2 = c(T(p)) + v_{p,2} + 1$.

This family will form a base case for the general recursion in the subsequent section. As noted above, there is a recursive structure here but with some ‘errors’ in the full decomposition. If the tile sizes are reduced to avoid these errors, then later tiles will be too small to cover \mathbb{Z}^2 .

Since these errors are limited to the degenerate family and the odometers for this family are so simple, we take the cumbersome but elementary approach and provide the exact formulas. One could avoid this by adding additional cases to the general recursion, however, a benefit here is that we can easily show these base cases satisfy a slightly stronger recurrence property as specified exactly in the last subsection. We then use this property to show recurrence inductively in the general recursion.

6.1. Base points. We first check that the base points of the hyperbola $0/1$ and $1/1$, are on $\partial\Gamma_F$ via an explicit construction. We recall a criteria for checking recurrence from the sandpile literature. Let $s : \mathbb{Z}^2 \rightarrow \mathbb{Z}$ and let H be a finite induced subgraph of the F -lattice. H is *allowed* for s if there is a vertex v of H where $s(v)$ is at least the in-degree of v in H and otherwise is *forbidden*.

Proposition 6.2. [HLM⁺08] *An integer superharmonic function g is recurrent if and only if every nonempty induced subgraph of the F -lattice is allowed for $s := \Delta g + 1$.*

In particular, Proposition 6.2 reduces verifying recurrence of a function to checking a condition on its Laplacian (which is no surprise given the function s in the statement is usually referred to as a recurrent sandpile [LP10]).

Lemma 6.1. *The functions*

$$g_{0/1}(x) = -\frac{x_2(x_2 + 1)}{2} \quad g_{1/1}(x) = -\lfloor \frac{(x_2 - x_1)^2}{4} \rfloor$$

are odometers for $0/1$ and $1/1$ respectively.

Proof. The growth condition can be checked using the definition (2). Moreover, $\Delta g_{0/1}(x) = \Delta g_{1/1}(x) = -1\{(x_1 + x_2) \text{ is even}\}$. By Proposition 6.2 it remains to check that every nonempty induced subgraph H of the F -lattice is allowed for $s = 1\{(x_1 + x_2) \text{ is odd}\}$. Let x denote the lower left vertex of H . That is x has minimal x_2 coordinate and of all other $y \in H$ with $y_2 = x_2$, x_1 is minimal. This implies the only possible neighbors of x in H are $x + e_1$ or $x + e_2$. If $(x_1 + x_2)$ is odd, then, $s(x) = 1$ so we may suppose otherwise. If $(x + e_1) \in H$, then $s(x + e_1) = 1$ and by the location of x , $(x + e_1 - e_2) \notin H$, thus $s(x + e_1)$ is larger than its in-degree in H , completing the proof. \square

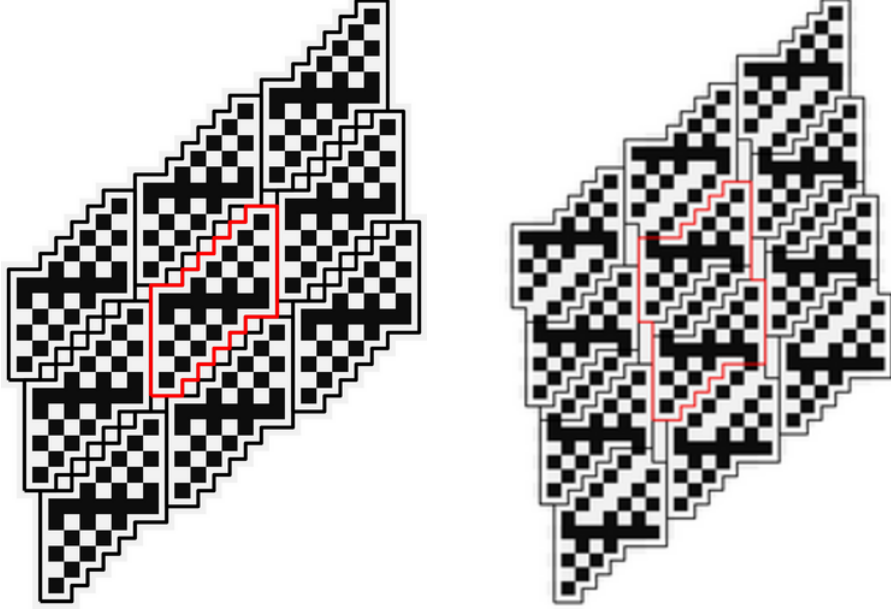


FIGURE 16. A period of the Laplacian of a staircase odometer on the left and its alternate. The string is 22 and the fraction is $3/4$. Each tile is outlined in the dual lattice.

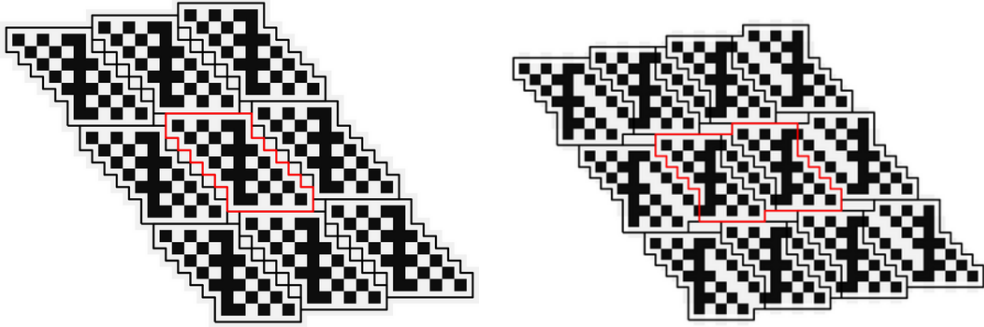


FIGURE 17. The rotated standard and alternate staircase odometers of Figure 16. The string is 33 and the fraction is $1/7$.

6.2. Staircases. The *staircase* fractions are the reduced fractions of the form $\frac{1}{d}$ for d odd and their rotations, $\mathcal{R}(1, d) = (\frac{d-1}{2}, \frac{d+1}{2})$. These fractions are the even child or odd child in Farey quadruples with words 3^k or 2^k for $k \geq 0$ respectively. As the construction will indicate, the tiles and Laplacians of odometers will be rotated versions of each other.

We start with the even child.

Lemma 6.2. *For each $d \geq 3$ odd, there is a unique function $g_{1/d} : \mathbb{Z}^2 \rightarrow \mathbb{Z}$ with*

$$g_{1/d}(x) = -\frac{1}{2}x_2(x_2 + 1) + (x_2 + \min(x_1 - 1, 0)) + 1\{x \in \{(0, 0), (2, d + 1)\}\} \quad \text{for } x \in T_{1/d}$$

where

$$T_{1/d} := \{(x_1, x_2) \in [2 - d, d] \times [0, d + 1] : 1 \leq (x_1 + x_2) \leq (d + 2)\} \cup \{(0, 0), (2, d + 1)\}$$

and

$$g_{1/d}(x \pm (d, 1)) = g_{1/d}(x) \quad \text{for } x \in \mathbb{Z}^2$$

$$g_{1/d}(x - (1 - d, 1 + d)) = g_{1/d}(x) - (1, -d) \cdot x - \left(\frac{1}{2}d(d+1) - 1\right) \quad \text{for } x \in \mathbb{Z}^2$$

$$g_{1/d}(x + (1 - d, 1 + d)) = g_{1/d}(x) + (1, -d) \cdot x - \left(\frac{1}{2}(d+1)(d+2) - 1\right) \quad \text{for } x \in \mathbb{Z}^2.$$

The odd child corresponding to 3^k is $1/d$ for d odd. On $T_{1/d}$, $g_{1/d}$ respects a qp^{k+1} horizontal boundary string and a $p^{2(k+1)}q$ vertical boundary string and their reversals. This fills the boundary.

Proof. From the definition of $T_{1/d}$, we see, using the notation of Lemma 4.1, that its boundary word is described by $w_1 = 1^d$ and $w_2 = (i * i) * (-1 * i)^{d-2} * i$. Therefore, by Lemma 4.1, the translations of $T_{1/d}$ by $\pm(d, 1)$ and $\pm(1 - d, 1 + d)$ generate an almost pseudo-square tiling. In particular, the translations cover \mathbb{Z}^2 . Therefore it suffices to check consistency of the first condition and the last three.

We do this by showing that the boundary of $T_{1/d}$ decomposes into four pieces which are exactly zero-one boundary strings which $g_{1/d}$ respects.

We start by observing, using the notation of the zero-one boundary string section that the bottom boundary of $T_{1/d}$ is qp^{k+1} zero-one reversed horizontal boundary string where $k+1 = (d-1)/2$. Indeed,

$$T_{1/d} \supset A_1 \cup A_2 := \{[0, 1] \times [0, 1]\} \cup \{[2, d] \times [0, 2]\}$$

is a qp^{k+1} horizontal boundary string:

$$A_1 = T_{1/1} \quad A_2 = v_{p,1} + \cup_{j=1}^{k+1} (T_{0/1} + jv_{p,1})$$

Moreover an inspection of the formula shows that $g_{1/d} = o_{1/1}$ on A_1 and $g_{1/d} = o_{0/1}$ on each translation of $T_{0/1}$.

The top boundary of $T_{1/d}$ is a $p^{k+1}q$ zero-one horizontal reversed boundary string. Indeed,

$$T_{1/d} \supset A_2^r \cup A_1^r := \{[2 - d, 0] \times [d - 1, d + 1]\} \cup \{[1, 2] \times [d, d + 1]\}$$

is a $p^{k+1}q$ zero-one reversed horizontal boundary string:

$$A_2^r = \cup_{j=0}^k \{T_{0/1} + jv_{p,1}\} \quad A_1^r = T_{1/1} + kv_{p,1} + v_{q,1} + 1.$$

To check that $g_{1/d}$ respects the string, it is convenient to consider the translation

$$g_{1/d}^r = g_{1/d} - (1, -d) \cdot x - \frac{1}{2}d(d+1) + 1$$

and recall the translated versions of the zero-one odometers, $\hat{o}_{1/1}$ and $\hat{o}_{0/1}$ defined previously on the reversed string. Once we make this translation, we can use the formula to compute

$$g_{1/d}^r([1, 2] \times [d, d + 1]) = \hat{o}_{1/1} = \begin{bmatrix} 0 & 0 \\ 0 & -1 \end{bmatrix}$$

and $g_{1/d}^r([2 - d, 0] \times [d - 1, d + 1]) = 0$ and $g_{1/d}^r([2 - d, 0], d - 1) = -1$ which coincides with $\hat{o}_{0/1}$ on each tile.

To show that this implies compatibility in the $\pm v_2$ direction, we need to show that $T_{1/d} \pm v_2$ the shared interface between $T_{1/d} \pm v_2$ is a stacked boundary string and the odometers respect the stack. To see that the shared interface is a boundary string, we need to show that the

offset between the two first tiles in the strings are $v_{p,2} + i$. As we defiend it above in the same tile, $c(T_{1//1,1}) = 0$ and for the reversed string $c(T_{0//1,1}) = 2 - d + (d - 1)i$. Thus, after translation by $(-1 + d) - (1 + d)i$ we get $-1 - 2i = -v_{p,2} - i$. To see that the odometers respect the stack, we observe that the affine translation makes the slope difference between the first two tiles $-a_{p,2}$.

The check for the vertical boundaries proceeds by comparing to the explicit formulas for the degenerate zero-one strings as specified previously. □

Then the odd child.

Lemma 6.3. *For each $p = \frac{d-1}{\frac{d+1}{2}}$, $d \geq 3$ odd, there is a unique function $g_p : \mathbb{Z}^2 \rightarrow \mathbb{Z}$ with*

$$g_p(x) = -\lfloor \frac{(x_2 - x_1)^2}{4} \rfloor + \min(d - x_2, 0) + 1\{x \in \{(0, d + 1), (d + 1, d - 1)\}\} \quad \text{for } x \in T_p$$

where

$$T_p := \{(x_1, x_2) \in [0, d + 1] \times [1, 2d - 1] : -1 \leq (x_2 - x_1) \leq d\} \cup \{(0, d + 1), (d + 1, d - 1)\}$$

and

$$g_p(x \pm (d + 1, d - 1)) = g_p(x) \quad \text{for } x \in \mathbb{Z}^2$$

$$g_p(x - (-1, d)) = g_p(x) - \left(\frac{d-1}{2}, \frac{d+1}{2}\right) \cdot x - \left(\lfloor \frac{(d+1)^2}{4} \rfloor - 1\right) \quad \text{for } x \in \mathbb{Z}^2$$

$$g_p(x + (-1, d)) = g_p(x) + \left(\frac{d-1}{2}, \frac{d+1}{2}\right) \cdot x - \left\lfloor \frac{(d+1)^2}{4} \right\rfloor \quad \text{for } x \in \mathbb{Z}^2.$$

On T_p , g_p respects a $q^{2(k+1)}p$ horizontal and a $pq^{(k+1)}$ vertical boundary string.

We next construct the alternate staircase odometers.

Lemma 6.4. *For each $d \geq 3$ odd, there is a unique function $\hat{g}_{1/d} : \mathbb{Z}^2 \rightarrow \mathbb{Z}$ with*

$$\begin{aligned} \hat{g}_{1/d}(x) = & -\frac{1}{2}x_2(x_2 + 1) + \min(0, 2 - x_1) + \min(0, d - 2 + x_1) \quad \text{for } x \in \hat{T}_d \\ & + \max(x_1 + x_2 - 2, 0) + 1_{A \cup B} \end{aligned}$$

where

$$A = \{-(d - 1) \times [-1, 0]\} \cup \{3 \times [d, d + 1]\}$$

$$B = \{(x_1, x_2) : (x_1 + x_2) = 2 \text{ and } 0 < x_2 < d\}$$

$$C = \{-1 \times [1 - d, 0]\} \cup \{(d + 1) \times [4 - d, 3]\}$$

$$D = \{(x_1, x_2) \in [4 - 2d, d] \times [0, d] : -d + 2 \leq x_1 + x_2 \leq d + 2\}$$

$$\hat{T}_{1/d} = A \cup B \cup C \cup D$$

and

$$\hat{g}_{1/d}(x \pm (d, 1)) = \hat{g}_{1/d}(x) \quad \text{for } x \in \mathbb{Z}^2$$

$$\hat{g}_{1/d}(x - (1 - d, 1 + d)) = \hat{g}_{1/d}(x) - (1, -d) \cdot x - \left(\frac{1}{2}d(d + 1) - 2\right) \quad \text{for } x \in \mathbb{Z}^2$$

$$\hat{g}_{1/d}(x + (1 - d, 1 + d)) = \hat{g}_{1/d}(x) + (1, -d) \cdot x - \frac{1}{2}(d + 1)(d + 2) \quad \text{for } x \in \mathbb{Z}^2.$$

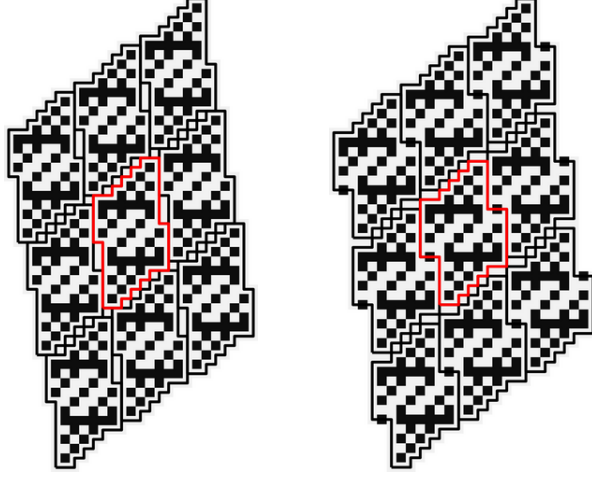


FIGURE 18. A period of the Laplacian of a doubled staircase odometer on the left and its alternate. The string is 22 and the reduced fraction is $5/7$. Each tile is outlined in the dual lattice.

The horizontal boundary of $\hat{g}_{1/d}$ respects a qp^{k+1} horizontal boundary string.

Then, the odd child.

Lemma 6.5. For each $p = \frac{d-1}{\frac{d+1}{2}}$, $d \geq 3$ odd, there is a unique function $\hat{g}_p : \mathbb{Z}^2 \rightarrow \mathbb{Z}$ with

$$\begin{aligned} \hat{g}_p(x) = & -\lfloor \frac{(x_2 - x_1)^2}{4} \rfloor + \min(d - x_2 - 1, 0) + \min((2d - 1) - x_2, 0) \quad \text{for } x \in \hat{T}_p \\ & + \max((x_2 - x_1) - d + 1, 0) + 1_{A \cup B} \end{aligned}$$

where

$$\begin{aligned} A &= \{[-1, 0] \times 2d\} \cup \{[d, d+1] \times d-2\} \\ B &= \{(x_1, x_2) : (x_2 - x_1) = d-1 \text{ and } 0 < x_1 < d\} \\ C &= \{-1 \times [d+1, 2d]\} \cup \{(d+1) \times [d-2, 2d-3]\} \\ D &= \{(x_1, x_2) \in [0, d] \times [1, 3d-3] : -1 \leq x_2 - x_1 \leq 2d-1\} \\ \hat{T}_p &= A \cup B \cup C \cup D \end{aligned}$$

and

$$\hat{g}_p(x \pm v_{p,i}) = \hat{g}_p(x) \pm a_{p,i} \cdot x + k_{p,i} \quad \text{for } x \in \mathbb{Z}^2,$$

where $k_{p,\pm i} \in \mathbb{Z}$ is a constant and $i \in \{1, 2\}$ selects the lattice vector. The vertical boundary respects a pq^{k+1} boundary string where p is omitted.

Lemma 6.6. The Laplacians are rotations of each other and have this formula.

6.3. Doubled staircases. The *doubled staircases* are the reduced fractions of the form $\frac{1}{d}$ for $d \geq 4$ even and their rotations $\mathcal{R}(1, d) = (d-1, d+1)$. These are respectively the odd or even child in Farey quadruples with words 3^k and 2^k for $k \geq 1$. They are the sibling of the opposite parity of the staircases.

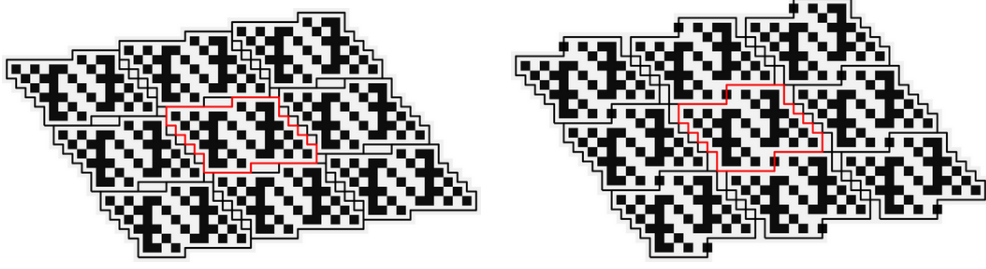


FIGURE 19. The rotated standard and alternate doubled staircase odometers of Figure 18. The string is 33 and the reduced fraction is $1/6$.

Lemma 6.7. *For each $d \geq 4$ even, there is a unique function $g_{1/d} : \mathbb{Z}^2 \rightarrow \mathbb{Z}$ with*

$$g_{1/d}(x) = -\frac{1}{2}x_2(x_2 + 1) + \min(0, x_1 - 1) + \min(0, d + 1 - x_1) \quad \text{for } x \in T_{1/d} \\ + \max((x_2 + x_1) - d - 1, 0) + 1_{A \cup B}$$

where

$$A = (0, -1) \cup (d + 2, d + 1)$$

$$B = \{(x_1, x_2) : (x_1 + x_2) = (d + 1) \text{ and } 0 < x_2 < d\}$$

$$C = \{(x_1, x_2) \in [-d + 2, 2d] \times [-1, d + 1] : 0 \leq (x_1 + x_2) \leq 2d + 2\}$$

$$D = \{(x_1, x_2) : x_1 \geq d \text{ and } x_2 = -1 \text{ or } x_1 \leq 2 \text{ and } x_2 = d + 1\}$$

$$T_{1/d} := \{A \cup B \cup C\} \setminus D$$

and

$$g_{1/d}(x \pm v_{1/d,i}) = g_{1/d}(x) \pm a_{1/d,i} \cdot x + k_{1/d,\pm i} \quad \text{for } x \in \mathbb{Z}^2,$$

where $k_{d,\pm i}$ is a constant and $i \in \{1, 2\}$ selects the lattice vectors.

Moreover, $g_{1/d}$ respects a $qp^k qp^{k+1}$ horizontal boundary string and a $p^{(2k+1)q}$ vertical boundary string.

Lemma 6.8. *For each $q = \frac{d-1}{d+1}$ $d \geq 4$ even, there is a unique function $g_q : \mathbb{Z}^2 \rightarrow \mathbb{Z}$ with*

$$g_q(x) = -\lfloor \frac{(x_2 - x_1)^2}{4} \rfloor + \min(0, d - x_2) + \min(0, 2d - x_2) \quad \text{for } x \in T_q \\ + \max((x_2 - x_1) - d, 0) + 1_{A \cup B}$$

where

$$A = (-1, 2d + 1) \cup (d + 1, d - 1)$$

$$B = \{(x_1, x_2) : (x_2 - x_1) = d \text{ and } 0 < x_1 < d\}$$

$$C = \{(x_1, x_2) \in [-1, d + 1] \times [1, 3d - 1] : -1 \leq (x_2 - x_1) \leq 2d + 1\}$$

$$D = \{(x_1, x_2) : x_1 = -1 \text{ and } x_2 \leq d + 1 \text{ or } x_1 = d + 1 \text{ and } x_2 \geq 2d - 1\}$$

$$T_q := \{A \cup B \cup C\} \setminus D$$

and

$$g_q(x \pm v_{q,i}) = g_q(x) \pm a_{q,i} \cdot x + k_{q,\pm i} \quad \text{for } x \in \mathbb{Z}^2,$$

where $k_{d,\pm i}$ is a constant and $i \in \{1, 2\}$ selects the lattice vectors.

Moreover, g_q respects a zero-one $q^{(2k+1)}p$ horizontal boundary string and a $pq^k pq^{(k+1)}$ vertical boundary string.

We next construct the alternates.

Lemma 6.9. *For each $d \geq 4$ even, there is a unique function $\hat{g}_{1/d} : \mathbb{Z}^2 \rightarrow \mathbb{Z}$ with*

$$\begin{aligned} \hat{g}_{1/d}(x) = & -\frac{1}{2}x_2(x_2 + 1) + \min(0, x_1) + \min(0, d - x_1 - 1) \quad \text{for } x \in \hat{T}_{1/d} \\ & + \max((x_2 + x_1) - d, 0) + 1_{A \cup B} \end{aligned}$$

where

$$\begin{aligned} A &= (-1, -1) \cup (d, d + 2) \\ B &= \{(x_1, x_2) : (x_1 + x_2) = (d) \text{ and } 0 < x_1 < d - 1\} \\ C &= \{(x_1, x_2) \in [-d + 1, 2d - 2] \times [-1, d + 2] : -1 \leq (x_1 + x_2) \leq 2d + 1\} \\ D &= \{(x_1, x_2) : x_1 \geq d \text{ and } x_2 \in [-1, 0] \text{ or } x_1 \leq -1 \text{ and } x_2 \in [d + 1, d + 2]\} \\ \hat{T}_{1/d} &:= \{A \cup B \cup C\} \setminus D \end{aligned}$$

and

$$\hat{g}_{1/d}(x \pm v_{1/d,i}) = \hat{g}_{1/d}(x) \pm a_{1/d,i} \cdot x + \hat{k}_{1/d,\pm i} \quad \text{for } x \in \mathbb{Z}^2,$$

where $\hat{k}_{d,\pm i}$ is a constant and $i \in \{1, 2\}$ selects the lattice vectors.

Moreover, $\hat{g}_{1/d}$ respects a horizontal zero-one $p^{(2k+1)}q$ boundary string and its reversal.

Lemma 6.10. *For each $q = \frac{d-1}{d+1}$, $d \geq 4$ even, there is a unique function $\hat{g}_q : \mathbb{Z}^2 \rightarrow \mathbb{Z}$ with*

$$\begin{aligned} \hat{g}_q(x) = & -\lfloor \frac{(x_2 - x_1)^2}{4} \rfloor + \min(0, d - x_2) + \min(0, 2d - 1 - x_2) \quad \text{for } x \in T_q \\ & + \max(0, x_2 - x_1 - d) + 1_{A \cup B} \end{aligned}$$

where

$$\begin{aligned} A &= (-2, 2d) \cup (d + 1, d - 1) \\ B &= \{(x_1, x_2) : (x_2 - x_1) = d \text{ and } 0 < x_1 < d\} \\ C &= \{(x_1, x_2) \in [-2, d + 1] \times [1, 3d - 2] : -1 \leq (x_2 - x_1) \leq 2d + 1\} \\ D &= \{(x_1, x_2) : x_1 \leq -1 \text{ and } x_2 \leq d + 1 \text{ or } x_1 \geq d \text{ and } x_2 \geq 2d\} \\ T_q &:= \{A \cup B \cup C\} \setminus D \end{aligned}$$

and

$$\hat{g}_q(x \pm v_{q,i}) = g_q(x) \pm a_{q,i} \cdot x + k_{q,\pm i} \quad \text{for } x \in \mathbb{Z}^2,$$

where $\hat{k}_{d,\pm i}$ is a constant and $i \in \{1, 2\}$ selects the lattice vectors.

Moreover, \hat{g}_q respects a zero-one $q^{(2k+1)}p$ horizontal boundary string and its reversal.

Lemma 6.11. *The Laplacians are rotations of each other and have the following formulas:*

6.4. Toppling highways and recurrence. In this section we prove that the staircase odometers and their doubles are recurrent. In fact, we prove something stronger which will allow us to prove recurrence later on inductively.

Lemma 6.12. *On the tile each sandpile is recurrent*

Proof. Use forbidden sub configurations. Slide a plane till it touches one side of the base. \square

Lemma 6.13. *Let $T(n/d)$ denote a standard tile described by the boundary word $w_1 w_2 \text{rev}(w_1) \text{rev}(w_2)$. If the corner corresponding to $w_1 w_2$ is fired, then all sites along w_1 and w_2 fire. The same holds for the flipped corner.*

Lemma 6.14. *For alternates, only the outer subtiles fire if the corners are fired. However, if one site in a ‘strip’ fires, then everything does.*

7. ODOMETERS AND TILES

This section extends the hyperbola recursion of Section 3 to all odometers and tiles. That is, we associate to each rational in a Farey quadruple a pair of tiles and odometers. For continuity of the literature, the formality which we use to define the recursion is similar to [LPS16].

7.1. Standard tiles. Let $(p_0, q_0) = \mathcal{C}(p_1, q_1)$ form a Farey quadruple labeled by $w \in F_3$. Let \mathcal{W}_1 count the number of 1s in w .

Definition 3. *A pair of tiles $(T(p_0), T(q_0)) \subset \mathbb{Z}^2$ are standard tiles for (p_0, q_0) if they appear in Proposition 6.1, are $(T_{0/1}, T_{1/1})$ from Section 5.4, or have the standard tile decomposition:*

$$(51) \quad \begin{aligned} T(p_0) &= T(p_1)^+ \cup T(p_1)^- \cup T^d(q_1)^+ \cup T^d(q_1)^- \\ T(q_0) &= T^d(p_1)^+ \cup T^d(p_1)^- \cup T(q_1)^+ \cup T(q_1)^- \end{aligned}$$

where $T^d(n/d)^\pm$ denote doubled tiles,

$$(52) \quad \begin{aligned} T^d(p)^\pm &= T(p)^{\pm,1} \cup T(p)^{\pm,2} := T(p) \cup (T(p) + v_{p,2}) \\ T^d(q)^\pm &= T(q)^{\pm,1} \cup T(q)^{\pm,2} := T(q) \cup (T(q) + v_{q,1}) \end{aligned}$$

and $(T(p_1), T(q_1))$, with or without superscripts, are standard tiles for (p_1, q_1) . The tile positions in (51) depend on the parity of \mathcal{W}_1 : if \mathcal{W}_1 is odd

$$(53) \quad \begin{aligned} c(T) - c(T(p_0)) &= \begin{cases} 0 & \text{if } T = T(p_1)^+ \\ 2v_{q_1,1} + v_{q_1,2} & \text{if } T = T(p_1)^- \\ 2v_{p_1,1} & \text{if } T = T^d(q_1)^+ \\ v_{p_1,2} & \text{if } T = T^d(q_1)^- \end{cases} \\ c(T) - c(T(q_0)) &= \begin{cases} 0 & \text{if } T = T^d(p_1)^+ \\ v_{q_1,1} + v_{q_1,2} & \text{if } T = T^d(p_1)^- \\ 2v_{p_1,1} & \text{if } T = T(q_1)^+ \\ 2v_{p_1,2} & \text{if } T = T(q_1)^- \end{cases} \end{aligned}$$

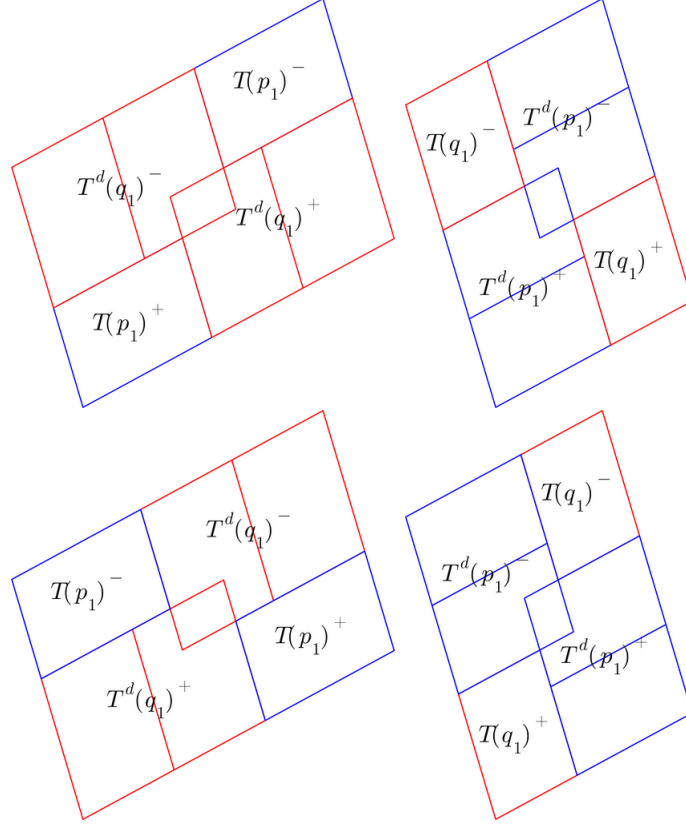


FIGURE 20. The two possible orientations for a standard tile pair from Definition 3. The left column is the odd child and the right column is the even child. The first row is the odd-first orientation and the second is the even-first orientation. Only one type of overlap between parents (corresponding to Type 1 children) is displayed - see Figure 21 for the other types of overlaps.

otherwise

$$(54) \quad \begin{aligned} c(T) - c(T(p_0)) &= \begin{cases} 0 & \text{if } T = T^d(q_1)^+ \\ 2v_{p_1,1} + v_{p_1,2} & \text{if } T = T^d(q_1)^- \\ 2v_{q_1,1} & \text{if } T = T(p_1)^+ \\ v_{q_1,2} & \text{if } T = T(p_1)^- \end{cases} \\ c(T) - c(T(q_0)) &= \begin{cases} 0 & \text{if } T = T(q_1)^+ \\ 2v_{p_1,1} + v_{p_1,2} & \text{if } T = T(q_1)^- \\ v_{q_1,1} & \text{if } T = T^d(p_1)^+ \\ v_{q_1,2} & \text{if } T = T^d(p_1)^-, \end{cases} \end{aligned}$$

see Figure 20.

The tiles in the standard tile decomposition of $T(n/d)$ will be called subtiles of $T(n/d)$. The tile orientations in (53) and (54) will be referred to as the odd-first and even-first orientations respectively. We will also call a single tile in a pair of standard tiles a standard tile.

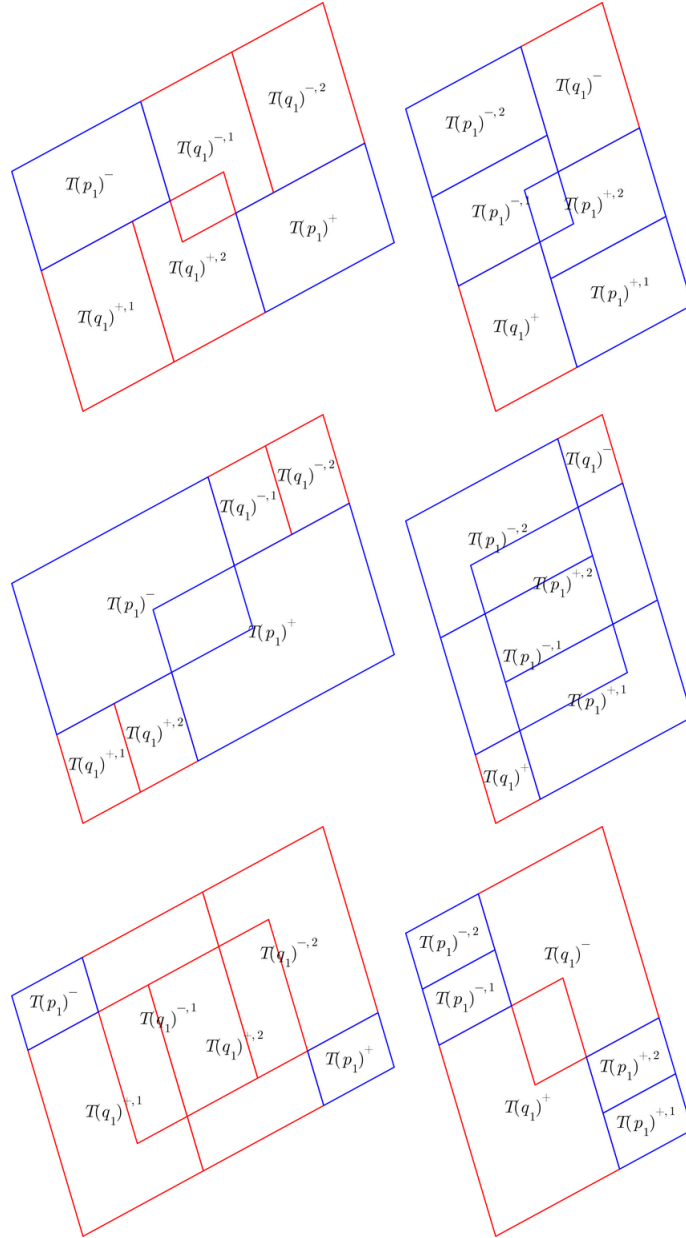


FIGURE 21. All possible overlaps between parents in a standard tile. The left column denotes the odd child and the right column is the even child. The rows from top to bottom correspond to Type 1, 2, then 3 children. The parent tiles are labeled in their centers with notation from Definition 3. The orientation is the even-first orientation.

Observe we have defined the recursion in a rotation invariant way. In particular, the horizontal edge of every tile is the vertical edge of some other tile. We make this precise in the next lemma by first proving that every tile indeed has ensures that odd standard tiles are sent to even standard tiles this will simplify the proof. We use the previous lemmas to

show that standard tiles periodically cover space and have certain compatibility properties. First, we prove a property of the boundary word of standard tiles.

Lemma 7.1. *If $0 < n/d < 1$, then the boundary word of $T(n/d)$ can be written as $w = w_1 * w_2 * \widehat{\text{rev}(w_1)} * \widehat{\text{rev}(w_2)}$ and w_1, w_2 satisfy the hypotheses in Lemma 4.1 and $\sum w_1 + i = v_{n/d,1}$ and $\sum w_2 - 1 = v_{n/d,2}$.*

Proof. The condition is true by Proposition 6.1 if $T(n/d)$ does not have a standard tile decomposition. Since every horizontal edge in those base cases is the vertical edge of some tile in the base cases and the standard decomposition also satisfies that property, it suffices to check the condition for w_1 .

We can rewrite the standard tile recursion to just produce w_1 . Let $str \in F_3$ be a word which expresses the quadruple. The bases cases are $str = 2^k$ for $k \geq 0$ and $str = 3^k$ for $k > 0$. In the base cases the explicit formula for the odd-even pair of edges (w_0, v_0) is

$$\begin{pmatrix} w_0 \\ v_0 \end{pmatrix} = \begin{cases} \begin{pmatrix} 1 * (1 * i)^{2k+1} * (1 * 1) \\ 1 * (1 * i)^{2k} (1 * 1) \end{pmatrix} & \text{if } str = 2^k \text{ for } k \geq 0 \\ \begin{pmatrix} (1 * 1)^k (1 * i) * (1 * 1)^{k+1} * 1 \\ 1 * (1 * 1)^{k+1} \end{pmatrix} & \text{if } str = 3^k \text{ for } k > 0 \end{cases}$$

The recursion is

$$\begin{pmatrix} w_{t+1} \\ v_{t+1} \end{pmatrix} = \begin{cases} \begin{pmatrix} w_t * i * v_t * i * v_t \\ w_t * i * v_t \end{pmatrix} & \text{if } \sum(str[i] = 1) \text{ is odd} \\ \begin{pmatrix} v_t * i * v_t * w_t \\ v_t * i * w_t \end{pmatrix} & \text{if } \sum(str[i] = 1) \text{ is even} \end{cases},$$

where w_t, v_t are the edges of the odd-even parents of str .

We can also get rid of the i but adding on an extra i to the base cases and being careful to remember that this recursion generates the bottom edge plus an i .

$$\begin{pmatrix} w_0 \\ v_0 \end{pmatrix} = \begin{cases} \begin{pmatrix} 1 * (1 * i)^{2k+1} * (1 * 1 * i) \\ 1 * (1 * i)^{2k} (1 * 1 * i) \end{pmatrix} & \text{if } str = 2^k \text{ for } k \geq 0 \\ \begin{pmatrix} (1 * 1)^k (1 * i) * (1 * 1)^{k+1} * 1 * i \\ 1 * (1 * 1)^{k+1} * i \end{pmatrix} & \text{if } str = 3^k \text{ for } k > 0 \end{cases}$$

The recursion is

$$\begin{pmatrix} w_{t+1} \\ v_{t+1} \end{pmatrix} = \begin{cases} \begin{pmatrix} w_t * v_t * v_t \\ w_t * v_t \end{pmatrix} & \text{if } \sum(str[i] = 1) \text{ is odd} \\ \begin{pmatrix} v_t * v_t * w_t \\ v_t * w_t \end{pmatrix} & \text{if } \sum(str[i] = 1) \text{ is even} \end{cases},$$

where again w_t, v_t are the edges of the odd-even parents of str .

$\text{str} = 2^k * \text{str}'$ for $k \geq 0$, $\text{str}[1] \neq 3$. In this case, write

$$\begin{pmatrix} p \\ q \end{pmatrix} = \begin{pmatrix} 1 * (1 * i)^{2k+1} * (1 * 1 * i) \\ 1 * (1 * i)^{2k} (1 * 1 * i) \end{pmatrix}$$

One can show that the recursion is an almost palindrome with letters p, q . If $\text{str}'[1] = 3$, one of the letters corresponds to the previous generation. But, even with a relabelling, the argument in the old notes shows that the recursion preserves the almost palindrome property.

That is, every word is of the form $p * \tilde{w} * q$ where \tilde{w} is a palindrome in the letters p, q .

Furthermore, $\tilde{p}i = ip$, in the letters $1, i$. This also holds for q . One can use this to check that either case (a) holds or case(b) holds in the letters $1, i$.

$\text{str} = 3^k * \text{str}'$ for $k > 0$. In this case, take the letters

$$\begin{pmatrix} p \\ q \end{pmatrix} = \begin{pmatrix} (1 * 1)^k * (1 * i) * (1 * 1)^{k+1} * 1 * i \\ 1 * (1 * 1)^{k+1} \end{pmatrix}$$

Also check that, $\tilde{p}i = ip$, in the letters $1, i$. This also holds for q . So, similar to the last part, we are in case (c). □

The next lemma uses the recursion on binary words in (26). For notational convenience, write $w_h(n/d)$ for the binary word associated to the reduced fraction in (26) with initial seed $w_0 = \{\}$ and $\mathbf{Q}_{\{\}} = (qqp, qp, p, q)$. Also write $w_v(n/d) = \mathcal{F}(w_h(\mathcal{R}(n/d)))$.

Lemma 7.2. *A standard tile, $T(n/d)$ exists for every reduced rational $0 \leq \frac{n}{d} \leq 1$. Moreover, when $0 < n/d < 1$, the tile has the following properties.*

- (1) $T(n/d)$ generates a $(v_{n/d,1}, v_{n/d,2})$ -regular almost pseudo-square tiling.
- (2) Each $T(n/d)$ is a $(w_h(n/d), w_v(n/d))$ -pseudo-square with offsets respecting the tiling:
 - (a) $c(T) - c(T(n/d)) = v_{n/d,1} - (i + 1)$ where T is the last tile of $w_h(n/d)$
 - (b) $c(T') - c(T(n/d)) = v_{n/d,2} - (2i - 1)$ where T' is the last tile of $\text{rev}(w_v(n/d))$
- (3) The surrounding of $T(n/d)$ with respect to $(v_{n/d,1}, v_{n/d,2})$ consists of two stacked zero-one horizontal and two vertical boundary strings.
- (4) When $T(n/d)$ has a standard decomposition, the shared boundary between neighboring subtiles is part of or is a stacked horizontal or vertical zero-one boundary string.

Proof. In light of Proposition 6.1, we may assume $T(n/d)$ has a standard decomposition and the statements are true for its parents, $T(p_1)$ and $T(q_1)$. Also, by Lemma 7.1 to prove part (a) it suffices to show that $T(n/d)$ does not have any internal gaps. This will follow from part (c) and the zero-one-boundary string no gaps, hence we prove parts (b) and (c). We assume that the decomposition given is in the even-first orientation, otherwise flip the subsequent statements.

Step 1: (b)

By the inductive hypothesis, $T(p_1)$ and $T(q_1)$ are $(w_h(p_1), w_v(p_1))$ and $(w_h(q_1), w_v(q_1))$ pseudo-squares. Suppose $T(n/d)$ is odd and let T be the last tile in $T(q_1)^{+,1}$ and T' the first tile in $T(q_1)^{+,2}$. By definition T is a translation of $T(0/1)$ and T' a translation of $T(1/1)$. Moreover, by the definition of the standard decomposition and the inductive hypothesis on the offsets, $c(T') - c(T) = (1 + i)$, in particular, we can glue the two boundary strings

together. A similar argument applies to the interface between $T(q_1)^{+,2}$ and $T(p_1)$. This shows if (n/d) is odd, then $T(n/d)$ respects $w_h(q_1)w_h(q_1)w_h(p_1)$ otherwise it respects $w_h(q_1)w_h(p_1)$. A symmetric argument applies to the vertical boundary strings and a computation shows that the offsets respect the tiling.

Step 2: (c)

Let A be the horizontal string for $T(n/d)$ and B the reversed horizontal string for $T(n/d) - v_{n/d,2}$. Set $c(T(n/d)) = 0$. By part (b), the first tile in B is located at $c(T(n/d)) - v_{n/d,2} + v_{n/d,2} - (2i - 1)$. Thus, the offset between the first tile in B and the first tile in A is $2i - 1 = v_{0/1,2} + i$, the correct initial offset for a stacked string.

Similarly if C is the vertical string for $T(n/d)$ and D the reversed vertical string for $T(n/d) + v_{n/d,1}$, then the offsets between the first tiles is $(i + 1) = -v_{1/1,1}$. The other two sides are stacked strings by the above arguments for $T(n/d) - v_{n/d,1}$ and $T(n/d) + v_{n/d,2}$.

Step 3: (d)

We state the arguments with the aid of Figure 21. First consider the three possible boundaries between $T(q_1)^{+,1/2}$ and $T(p_1)^-$ when $T(n/d)$ is odd. By the inductive hypothesis and (3), the offset between the first tile in the reversed zero-one horizontal boundary string for $T(q_1)^{+,1}$ and the first tile for the zero-one horizontal string in $T(p_1)^-$ is $v_{0/1,2} + i$. Since the initial offset is correct, the rest of the interface forms part of a stacked horizontal zero-one boundary string by part (3) of Lemma 5.1. Indeed, every letter other than the first matches across the interface. Reversing the roles of p_1 and q_1 above shows the three possible interfaces between $T(p_1)^+$ and $T(q_1)^{-,1/2}$ also form part of a stacked horizontal boundary string. When $T(n/d)$ is even, the interface between $T(p_1)^{+,1}$ and $T(p_1)^{+,2}$ is exactly a stacked horizontal boundary string by part (c). By rotation, the above arguments apply to the vertical interfaces. \square

7.2. Weak standard odometers. Our current goal is to extend the standard tile decomposition to odometers. In order to do so, we must define the operation of doubling a partial odometer. However, in the course of the recursion, doubled odometers may need to be partially corrected in the interior of the tile so we need a notion of tile that only agrees on part of the boundary.

Definition 4. Let $T(n/d)$ be a $(w_h(n/d), w_v(n/d))$ pseudo-square. A partial tile $T^{h^\pm/v^\pm}(n/d)$ is a tile which is a subset of $T(n/d)$ and coincides with $T(n/d)$ on one of the four sides:

$$(55) \quad T^{h^\pm/v^\pm}(n/d) \cap T(n/d) = \begin{cases} w_h(n/d) & \text{case } h^+ \\ \mathbf{rev}(w_h(n/d)) & \text{case } h^- \\ w_v(n/d) & \text{case } v^+ \\ \mathbf{rev}(w_v(n/d)) & \text{case } v^- \end{cases}$$

We now define the notion of a doubled odometer using partial tiles.

Definition 5. For $(n/d) \in \{p_0, q_0\}$ let $T(n/d)$ be a standard tile and $T^{h^\pm/v^\pm}(n/d)$ a partial tile. Denote by

$$(56) \quad T^{d,p,\pm}(n/d) = T(n/d)^1 \cup T^{h^\pm/v^\pm}(n/d)^2 := T(n/d) \cup (T^{h^\pm/v^\pm}(n/d) + v_{n/d})$$

a subset of the doubled tile $T^d(n/d)$, where $v_{n/d} = v_{p,2}$ or $v_{n/d} = v_{q,1}$.

The weak doubling of a partial odometer $o_{n/d}$ with domain $T(n/d)$ is a partial odometer $d(o)_{n/d}^\pm : T^{d,p}(n/d) \rightarrow \mathbb{Z}$ with the decomposition

$$(57) \quad d(o)_{n/d}^\pm = o_{n/d} \cup o_{n/d}^*$$

where $T(o_{n/d}) = T(n/d)^1$ and $T(o_{n/d}^*) = T^{h^\pm/v^\pm}(n/d)^2$ and, after being restricted to the relevant zero-one boundary strings from Definition 4, $o_{n/d}^*$ is a translation of $o_{n/d}$ with affine offsets dictated by the translation.

We now use these to partially define the standard recursion. The full recursion will require alternate tiles odometers which we will define in the next two subsections.

Definition 6. A pair of partial odometers $o_{p_0} : T(p_0) \rightarrow \mathbb{Z}$ and $o_{q_0} : T(q_0) \rightarrow \mathbb{Z}$ are weak standard tile odometers for (p_0, q_0) if they appear in Proposition 6.1, are $(o_{0/1}, o_{1/1})$ from Section 5.4 or if $(T(p_0), T(q_0))$ are standard tiles with standard decompositions for (p_0, q_0) and the partial odometers have the standard decompositions:

$$(58) \quad \begin{aligned} o_{p_0} &= o_{p_1}^+ \cup o_{p_1}^- \cup d(o)_{q_1}^+ \cup d(o)_{q_1}^- \\ o_{q_0} &= d(o)_{p_1}^+ \cup d(o)_{p_1}^- \cup o_{q_1}^+ \cup o_{q_1}^- \end{aligned}$$

where $d(o)_{n/d}^\pm$ are the respective weak doublings.

The translations and affine factors are dictated by the tile decompositions in Definition 3. For example, if $c(T(o_{p_0})) - c(T(o_{p_1}^-)) = 2v_{q_1,1} + v_{q_1,2}$, then $s(o_{p_0}) - s(o_{p_1}^-) = 2a_{q_1,1} + a_{q_1,2}$.

We say weak standard tile odometers $o_{n/d}$ and $o'_{n/d}$ are lattice adjacent if

$$\begin{aligned} c(T(o_{n/d})) - c(T(o'_{n/d})) &= v_{i,1/2} \\ s(o_{n/d}) - s(o'_{n/d}) &= \pm a_{i,1/2}, \end{aligned}$$

for $i \in \{1, 2\}$. We now prove an analogue of Lemma 7.2 for weak standard odometers.

Lemma 7.3. A weak standard odometer, $o(n/d)$ exists for every reduced rational $0 \leq \frac{n}{d} \leq 1$. Moreover, when $0 < n/d < 1$, the odometer has the following properties.

- (a) $o(n/d)$ respects $(w_h(n/d), w_v(n/d))$
- (b) Let A, B, C, D denote the first and last tiles of $w_h(n/d)$ and the last and first tiles of $\mathbf{rev}(w_h)(n/d)$ respectively (geometrically a counter-clockwise walk around the tile). Let o_Z be the restriction of $o(n/d)$ to $Z \in \{A, B, C, D\}$. Then, $s(o_B) - s(o_A) = 0$, $s(o_C) - s(o_D) = a_{0/1,2} - a_{1/1,2}$ and $s(o_C) - s(o_B) = a_{n/d,2} - a_{1/1,2}$.
- (c) Lattice adjacent $o'_{n/d}$ and $o_{n/d}$ are compatible.

Proof. By Proposition 6.1, we may assume the tile $T(n/d)$ has a standard decomposition. We split the proof into steps.

Step 1: Existence

Suppose $T(n/d)$ is odd and let $o_{p_1}^+, o_{p_1}^-, d(o)_{q_1}^+, d(o)_{q_1}^-$ be weak standard odometers for the tiles in the decomposition. By possibly deleting part of the odometers in $d(o)_{q_1}^\pm$, we may assume that the only overlaps between the subodometers occurs on the internal zero-one boundary strings. Therefore, compatibility follows when we prove that the affine offsets between the boundary strings is correct. This follows from part (a) and (b) of the inductive hypothesis and the definition of zero-one boundary string.

Step 2. (a)

Induction and part (b)

Step 3. (b)

Definition of zero-one boundary string and part (a)

Step 4. (c) Definition of zero-one boundary string, the translation offsets, and part(b)

□

7.3. Alternate tiles. The tile recursion for alternates depends on the last letter of the word, in particular, the parents of the parents. If the last letter of the word is i , we say that we are in the Type i case. In case the word is empty, we say we are in the Type 1 case.

Definition 7. A pair of tiles $(\hat{T}(p_0), \hat{T}(q_0)) \subset \mathbb{Z}^2$ are alternate tiles for (p_0, q_0) if they have the alternate tile decomposition

$$(59) \quad \begin{aligned} \hat{T}(p_0) &= T^{ds}(q_1)^+ \cup T^{ds}(q_1)^- \cup T(p_1)^+ \cup T(p_1)^- \cup \hat{T}(q_1) \\ \hat{T}(q_0) &= T(q_1)^+ \cup T(q_1)^- \cup T^{ds}(p_1)^+ \cup T^{ds}(p_1)^- \cup \hat{T}(p_1) \end{aligned}$$

where $T^{ds}(n/d)^\pm$ denote doubled tiles where the doubling is different depending on the orientation:

$$(60) \quad \begin{aligned} T^{ds}(p)^\pm &= T(p)^{\pm,1} \cup T(p)^{\pm,2} := T(p) \cup (T(p) + S_p) \\ T^{ds}(q)^\pm &= T(q)^{\pm,1} \cup T(q)^{\pm,2} := T(q) \cup (T(q) + S_q), \end{aligned}$$

where

$$(61) \quad (S_p, S_q) = \begin{cases} (v_{q,1} + v_{p,2}, -v_{q,1} + v_{p,2}) & \text{if } \mathcal{W}_1 \text{ is even} \\ (-v_{q,1} + v_{p,2}, v_{q,1} + v_{p,2}) & \text{otherwise} \end{cases}$$

and $(T(p_1), T(q_1))$ with or without superscripts are standard tiles for (p_1, q_1) and $\hat{T}(n/d)$ is an alternate tile for n/d .

The standard tile positions in (59) depend on the parity of \mathcal{W}_1 : if \mathcal{W}_1 is odd

$$(62) \quad \begin{aligned} c(T) - c(\hat{T}(p_0)) &= \begin{cases} 2v_{p_1,1} & \text{if } T = T(q_1)^+ \\ 2v_{p_1,2} - v_{q_1,1} & \text{if } T = T(q_1)^- \\ 0 & \text{if } T = T^{ds}(p_1)^+ \\ v_{q_1,1} + v_{q_1,2} & \text{if } T = T^{ds}(p_1)^- \end{cases} \\ c(T) - c(\hat{T}(q_0)) &= \begin{cases} 2v_{p_1,1} & \text{if } T = T^{ds}(q_1)^+ \\ v_{p_1,2} & \text{if } T = T^{ds}(q_1)^- \\ 0 & \text{if } T = T(p_1)^+ \\ v_{p_1,2} + v_{q_1,2} + 2v_{q_1,1} & \text{if } T = T(p_1)^- \end{cases} \end{aligned}$$

otherwise

$$(63) \quad \begin{aligned} c(T) - c(\hat{T}(p_0)) &= \begin{cases} 0 & \text{if } T = T(q_1)^+ \\ 2v_{p_1,1} + 2v_{p_1,2} + v_{q_1,1} & \text{if } T = T(q_1)^- \\ v_{q_1,1} & \text{if } T = T^{ds}(p_1)^+ \\ v_{q_1,2} & \text{if } T = T^{ds}(p_1)^- \end{cases} \\ c(T) - c(\hat{T}(q_0)) &= \begin{cases} 0 & \text{if } T = T^{ds}(q_1)^+ \\ 2v_{p_1,1} + v_{p_1,2} & \text{if } T = T^{ds}(q_1)^- \\ v_{q_1,1} & \text{if } T = T(p_1)^+ \\ v_{p_1,2} + v_{q_1,2} - v_{q_1,1} & \text{if } T = T(p_1)^- \end{cases} \end{aligned}$$

The alternate tile positions in (59) may depend on both the parity of \mathcal{W}_1 , (even-first/odd-first) and the type of the child:

$$(64) \quad c(\hat{T}(q_1)) - c(\hat{T}(p_0)) = \begin{cases} v_{p_1,2} + 2v_{p_1,1} - v_{q_1,1} & \text{odd-first and Type 1 or 3} \\ *(v_{p_1,2}) & \text{odd-first and Type 2} \\ v_{q_1,1} + v_{p_1,2} & \text{even-first and Type 1 or 3} \\ *(v_{p_1,2} + v_{q_1,1}) & \text{even-first and Type 2} \end{cases}$$

$$(65) \quad c(\hat{T}(p_1)) - c(\hat{T}(q_0)) = \begin{cases} v_{p_1,2} + v_{q_1,1} & \text{odd-first and Type 1} \\ 2v_{q_1,1} + v_{q_1,2} & \text{odd-first and Type 2} \\ *(v_{q_1,1} + v_{p_1,2}) & \text{odd-first and Type 3} \\ v_{p_1,2} + 2v_{p_1,1} - v_{q_1,1} & \text{even-first and Type 1} \\ v_{q_1,2} & \text{even-first and Type 2} \\ *(v_{p_1,2} + v_{q_1,1} - 2(v_{q_1,1} - 2v_{p_1,1})) & \text{even-first and Type 3} \end{cases}$$

where in the cases indicated by $*$, the alternate tile may be omitted.

XX offsets in (2) is only done for the even-first orientation

Lemma 7.4. An alternate tile, $\hat{T}(n/d)$ exists for every reduced rational $0 \leq \frac{n}{d} \leq 1$. Moreover, when $0 < n/d < 1$, the tile has the following properties.

- (1) $\hat{T}(n/d)$ covers space under the lattice $L'(n/d)$
- (2) If n/d is even $\hat{T}(n/d)$ is a $w_h(n/d)$ -pseudo-square, otherwise a $w_v(n/d)$ pseudo-square with offsets respecting the tiling:
 - (a) Even case: $c(T_1) - c(T(n/d)) = 0$ where T_1 is first tile of $w_h(n/d)$ and
 - (b) Odd case: $c(T'_1) - c(T(n/d)) = 0$ where T'_1 is the first tile of $\mathbf{rev}(w_v(n/d))$
- (3) The surrounding of $\hat{T}(n/d)$ with respect to $(v_{n/d,1}, v_{n/d,2})$ consists of either part of a stacked zero-one boundary string or a complete overlap on a subtile.
- (4) When $\hat{T}(n/d)$ has an alternate decomposition, the shared boundary between neighboring subtiles is part of or is a stacked horizontal or vertical zero-one boundary string.

Proof. We may assume by Proposition 6.1 that $\hat{T}(n/d)$ has an alternate decomposition.

Suppose $\hat{T}(n/d)$ is even. Consider the enlarged tile with boundary word $w_1 = w_{q,1}w_{q,1}w_{p,2}$ and $w_2 = w_{p,2}w_{q,2}w_{p,2}$. Offset so that this boundary word passes over the boundary word of the tile and contains it. Call the enlarged tile Te

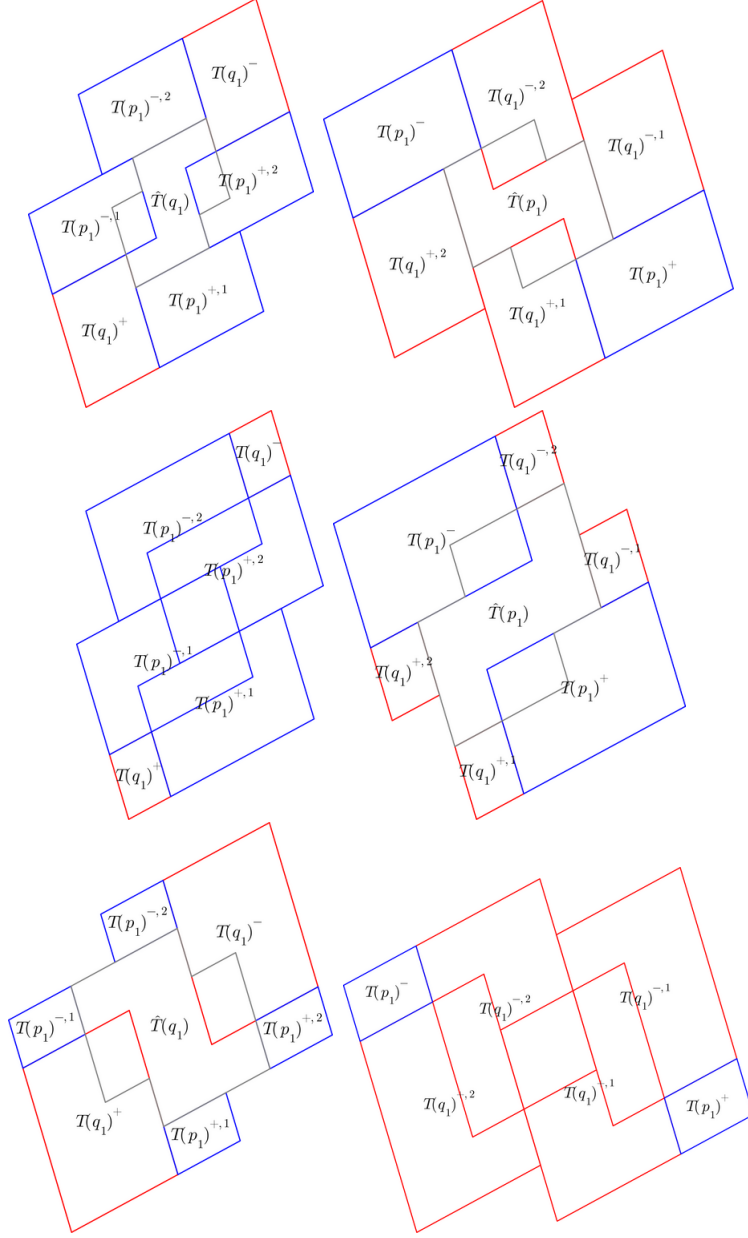


FIGURE 22. As Figure 21 (even-first) but for alternate tiles with labels from Definition 7.

This enlarged tile forms a regular $(\sum v_{n/d,1} + v_{q,1}, \sum v_{n/d,2})$ almost pseudo-square tiling. Conclude by the argument in Figure 24.

The rest of the proof is similar, substituting in boundary string words for boundary words. \square

7.4. Weak alternate odometers. The recursion for alternate odometers given the subtile placement is similar to the standard ones. To that end, we first extend the notion of doubled odometer to the shifted case

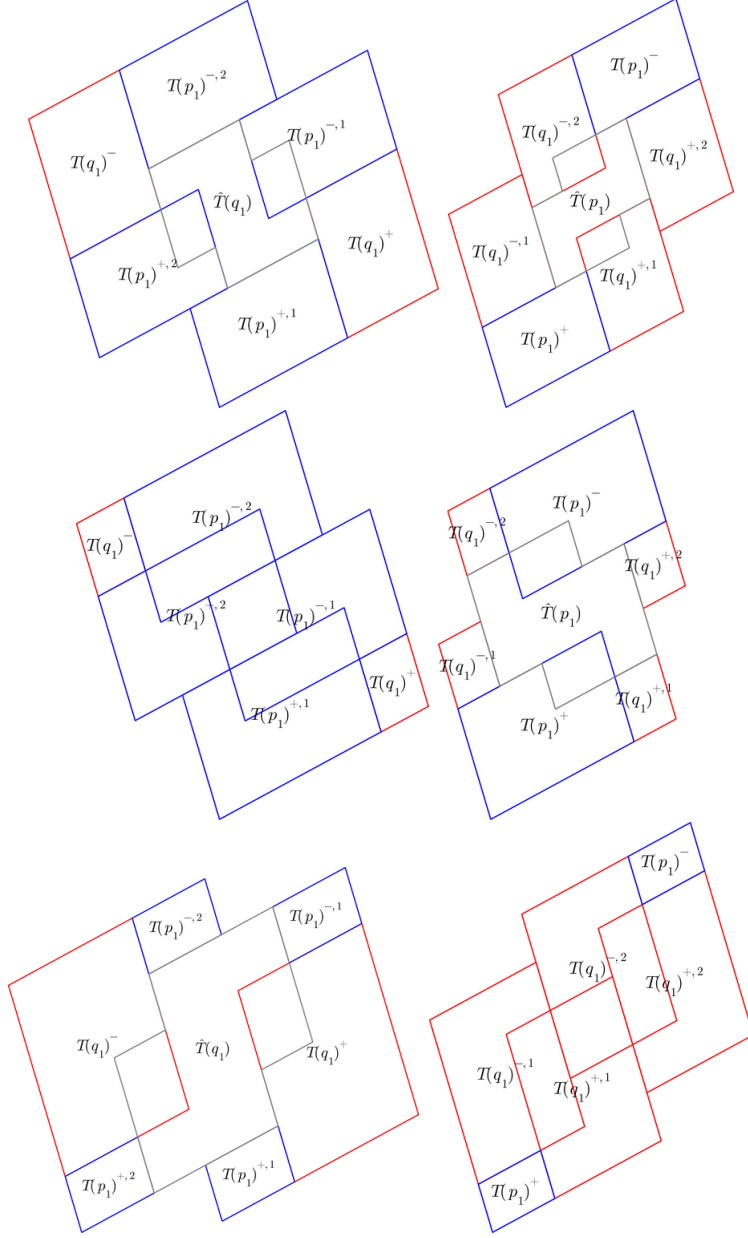


FIGURE 23. As Figure 22 but in the odd-first orientation

Definition 8. Let $T^{ds,h/v,\pm}(n/d) = T(n/d) \cup (T^{h/v,\pm}(n/d) \cup S_{n/d})$, a subset of $T^{ds}(n/d)$ from Definition 7, denote the analogue of Definition 5 with translation offsets specified by (60). Similarly extend the weak doubled odometer $ds(o)_{n/d} : T^{ds,h/v,\pm}(n/d) \rightarrow \mathbb{Z}$ (using standard odometers and enforcing the translation requirement on the boundary word tile). These will be called *shifted doublings*.

We are now ready to state a weak version of the alternate odometer recursion, analogous to the standard one from before.

Definition 9. A pair of partial odometers $\hat{o}_{p_0} : T(p_0) \rightarrow \mathbb{Z}$ and $\hat{o}_{q_0} : T(q_0) \rightarrow \mathbb{Z}$ are weak alternate tile odometers for (p_0, q_0) if they appear in Proposition 6.1, are $(o_{0/1}, o_{1/1})$ from

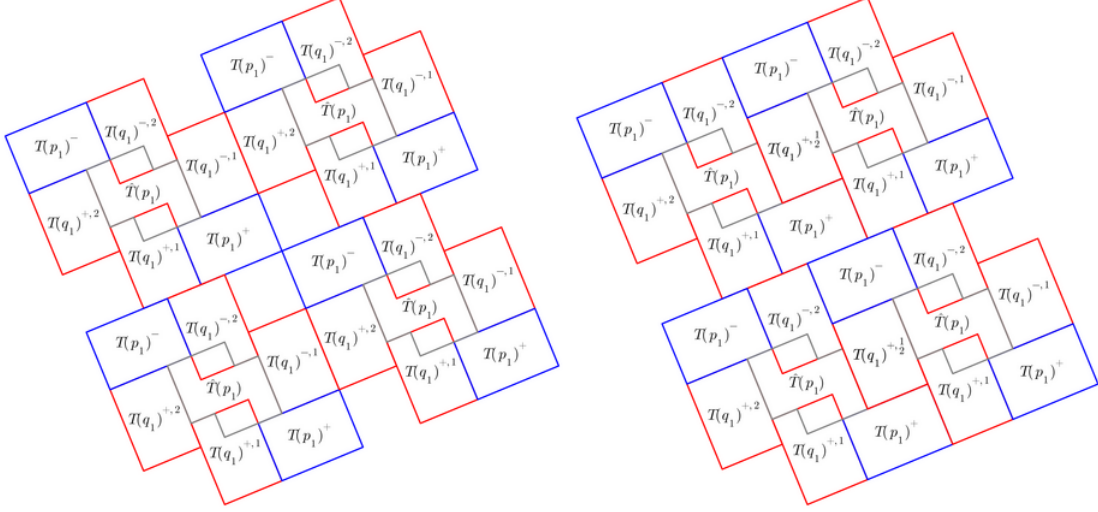


FIGURE 24. A visual explanation of the proof of Lemma 7.4. On the left is a portion of the shifted tiling $\hat{T}(n/d) \cup (\hat{T}(n/d) + v_{n/d,1} + v_{q,1}) \cup (\hat{T}(n/d) - v_{n/d,2}) \cup (\hat{T}(n/d) + v_{n/d,1} + v_{q,1})$ and on the right is a portion of the usual tiling $\hat{T}(n/d) \cup (\hat{T}(n/d) + v_{n/d,1}) \cup (\hat{T}(n/d) - v_{n/d,2}) \cup (\hat{T}(n/d) - v_{n/d,2} + v_{n/d,1})$.

Section 5.4 or $(\hat{T}(p_0), \hat{T}(q_0))$ are alternate tiles for (p_0, q_0) and the partial odometers have the decompositions:

$$(66) \quad \begin{aligned} \hat{o}_{p_0} &= ds(o)_{q_1}^+ \cup ds(o)_{q_1}^- \cup o_{p_1}^+ \cup o_{p_1}^- \cup \hat{o}(q_1) \\ \hat{o}_{q_0} &= o_{q_1}^+ \cup o_{q_1}^- \cup ds(o)_{p_1}^+ \cup ds(o)_{p_1}^- \cup \hat{o}(p_1) \end{aligned}$$

where $ds(o)_{n/d}^\pm$ and $\hat{o}(n/d)$ are the respective weak shifted doublings and weak alternate parent odometers.

As in Definition 6, the translations and affine factors are dictated by the tile decompositions in Definition 7.

Lemma 7.5. A weak alternate odometer, $\hat{o}(n/d)$ exists for every reduced rational $0 \leq \frac{n}{d} \leq 1$. Moreover, when $0 < n/d < 1$, the odometer has the following properties.

- (a) $\hat{o}(n/d)$ respects $w_h(n/d)$ or $w_v(n/d)$ if (n/d) is even or odd respectively.
- (b) Lattice adjacent $\hat{o}'_{n/d}$ and $\hat{o}_{n/d}$ are compatible.

Proof. By Proposition 6.1, we may assume the tile $\hat{T}(n/d)$ has an alternate decomposition. The proof then is similar to the standard case. First, delete part of the doubled odometers so that the overlaps between subodometers occur only on stacked zero-one boundary strings. Compatibility then follows once we check the affine offsets are correct. \square

In order to define odometers which exist in the interior of the a tile, we need to combine both alternates and standards to check that the internal overlaps match.

8. CORRECTING THE RECURSION

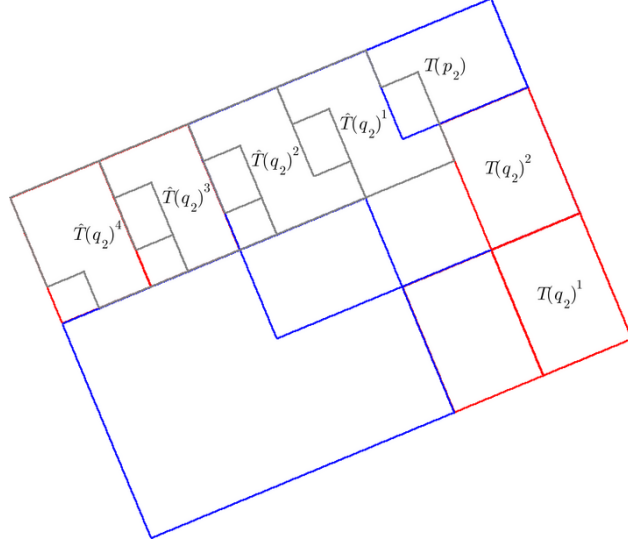


FIGURE 25. An odd L -correction with labels as in Definition 10 overlaid on its standard tile.

8.1. Corrected partial tiles and odometers. In this section we define a partial tile, Definition ??, for every standard tile which allows for four standard tiles to appear in the double decompositions. The construction of this partial tile will involve a chain of ancestor tiles which ‘corrects’ the recursion.

Let $(p_0, q_0) = \mathcal{C}(p_1, q_1)$ with recursion word $w \in F_3$ and recall the standard tile decomposition from Definition 3.

Definition 10 (Odd L -correction). *Suppose $w = w_1 * s * 2^k$ where $|w_1| \geq 0$, $s \in \{1, 3\}$, and $k \geq 0$. Let (p_2, q_2) be the child Farey pair corresponding to the string $w = w_1 * s$ and let $(T(p_2), T(q_2))$ be standard tiles for (p_2, q_2) and $\hat{T}(q_2)$ an alternate tile for q_2 .*

An L -correction for $T(p_0)$, $T^{L,\pm}(p_0)$ is a partial tile, $T^{v,\pm}(p_0)$ with the following decomposition

$$(67) \quad T^{L,\pm}(p_0) = \bigcup_{j=0}^k (T(q_2) + K_1 \cdot j) \cup (T(p_2) + K_2) \cup \left(K_3 + \bigcup_{i=1}^{2(k+1)-1\{s=3\}} (\hat{T}(q_2) + K_4 \cdot i) \right)$$

where the initial offset is specified by requiring $T(q_2)$ match an outer $T(q_1)$ tile in the standard decomposition:

$$\begin{cases} T(q_1)^{+,2} & 10 \\ T(q_1)^{-,1} & 11 \\ T(q_1)^{+,1} & 00 \\ T(q_1)^{-,2} & 01 \end{cases}$$

and the subsequent offsets are

$$[K_1, K_2] = \begin{cases} [v_{q_2,2}, v_{q_2,2} + (v_{q_2,1} - 2v_{p_2,1})] & 10 \\ [v_{q_2,2}, -v_{p_2,2}] & 11 \\ [v_{q_2,2}, v_{q_2,2}] & 00 \\ [-v_{q_2,2}, -v_{p_2,2} - (2v_{p_2,1} - v_{q_2,1})] & 01 \end{cases}$$

and

$$[K_3, K_4] = \begin{cases} [(-v_{q_2,2} + v_{p_2,2}) + (2v_{p_2,1} - v_{q_2,1}), -v_{q_2,1}] & 10 \\ [2v_{p_2,1} - v_{q_2,1}, v_{q_2,1}] & 11 \\ [-(v_{q_2,2} + v_{p_2,2}), v_{q_2,1}] & 00 \\ [0, -v_{q_2,1}] & 01, \end{cases}$$

where the right-hand side columns denote the case:

$$(68) \quad \begin{aligned} 10 &= \mathcal{W}_1 \text{ is odd and } + \\ 11 &= \mathcal{W}_1 \text{ is odd and } - \\ 00 &= \mathcal{W}_1 \text{ is even and } + \\ 01 &= \mathcal{W}_1 \text{ is even and } -. \end{aligned}$$

The correction in the even-case is similar but the offsets are slightly different due to the lack of rotational symmetry in the parameterization.

Definition 11 (Even L -correction). Suppose $w = w_1 * s * 3^k$ where $|w_1| \geq 0$, $s \in \{1, 2\}$, and $k \geq 0$. Let (p_2, q_2) be the child Farey pair corresponding to the string $w = w_1 * s$ and let $(T(p_2), T(q_2))$ be standard tiles for (p_2, q_2) and $\hat{T}(p_2)$ an alternate tile for p_2 .

An L -correction for $T(q_0)$, $T^{L,\pm}(q_0)$ is a partial tile $T^{h,\pm}(q_0)$ with the following decomposition.

$$(69) \quad T^{L,\pm}(q_0) = \bigcup_{j=0}^k (T(p_2) + K_1 \cdot j) \cup (T(q_2) + K_2) \cup \left(K_3 + \bigcup_{i=1}^{2(k+1)-1\{s=2\}} (\hat{T}(p_2) + K_4 \cdot i) \right)$$

where the initial offset is specified by requiring $T(p_2)$ match an outer $T(p_1)$ tile in the standard decomposition:

$$\begin{cases} T(p_1)^{+,1} & \{0 \text{ or } 1\}0 \\ T(p_1)^{-,2} & \{0 \text{ or } 1\}1 \end{cases}$$

and

$$[K_1, K_2, K_4] = \begin{cases} [2v_{p_2,1}, 2v_{p_2,1}, v_{p_2,2}] & 10 \\ [-2v_{p_2,1}, -v_{q_2,1}, v_{p_2,2}] & 00 \\ [-2v_{p_2,1}, -v_{q_2,1} + v_{p_2,1} - v_{q_2,1}, -v_{p_2,2}] & 11 \\ [2v_{p_2,1}, 2v_{p_2,1} + v_{p_2,2} - v_{q_2,2}, -v_{p_2,2}] & 01 \end{cases}$$

and

$$K_3 = \begin{cases} v_{q_1,1} - 2v_{p_1,1} + (v_{q_1,2} - v_{p_1,2} + v_{q_1,1}) & 10 \text{ and } s = 2 \\ v_{q_1,1} - 2v_{p_1,1} & 10 \text{ and } s = 1 \\ v_{q_1,2} - v_{p_1,2} & 00 \text{ and } s = 2 \\ 2v_{p_1,1} - v_{q_1,1} & 00 \text{ and } s = 1 \\ v_{q_1,2} - v_{p_1,2} + v_{q_1,1} & 11 \text{ and } s = 2 \\ 0 & 11 \text{ and } s = 1 \\ v_{q_1,2} - v_{p_1,2} - 2v_{p_1,1} + v_{q_1,1} & 01 \text{ and } s = 2 \\ 0 & 01 \text{ and } s = 2, \end{cases}$$

where the cases on the right are described by (68).

Note that the definitions assume that $T(p_2) = T(p_1)$ in the odd case and $T(q_2) = T(q_1)$ in the even case but this follows the standard tile decomposition or Proposition 6.1.

We extend the definition of corrected tiles to odometers.

Definition 12. Suppose the recursion word is from Definition 11 or 10. A weak L -correction for $o(n/d)$ is a partial odometer for $o^{h/v,\pm}(n/d) : T^{h/v,\pm}(n/d) \rightarrow \mathbb{Z}$ with decomposition into weak standard or weak alternate tile odometers respecting (69) if (n/d) is even and (67) otherwise.

Lemma 8.1. L corrected tiles are partial tiles and weak L corrected odometers exist.

Proof. The decomposition consists of lattice adjacent standard odometers or lattice adjacent alternate odometers and one of two possible new types of intersection seen in Figure 27. Since we have shown lattice adjacent odometers to be compatible (and that there are no gaps between lattice adjacent odometers), it suffices deal with the new intersection. This can be dealt with using the double decomposition, see 28. In particular, in the double decomposition, every pair of interfaces between the triple are part of or are a complete stacked zero-one boundary string. In case the triple comes from the base cases, you can check directly.

It remains to check that the appropriate zero-one boundary string is that of the standard tile. For that, we need to induct on k as the claim is immediate when $k = 0$. For $k \geq 1$, use the inductive hypothesis and the double decomposition. □

8.2. Tile odometers. A *tile odometer* is one of the base cases or is a weak tile odometer where the doubled odometer is possibly replaced by an L corrected odometer. An *L corrected tile odometer* is a weak L corrected odometer where the odometers in the chain decomposition are replaced by tile odometers.

No correction needed. This occurs whenever there is no overlap. We check that this is well-defined using the double decomposition.

Correction needed. Whenever there is a double overlap, replace the two weak standard odometers by complementary, \pm L -corrections.

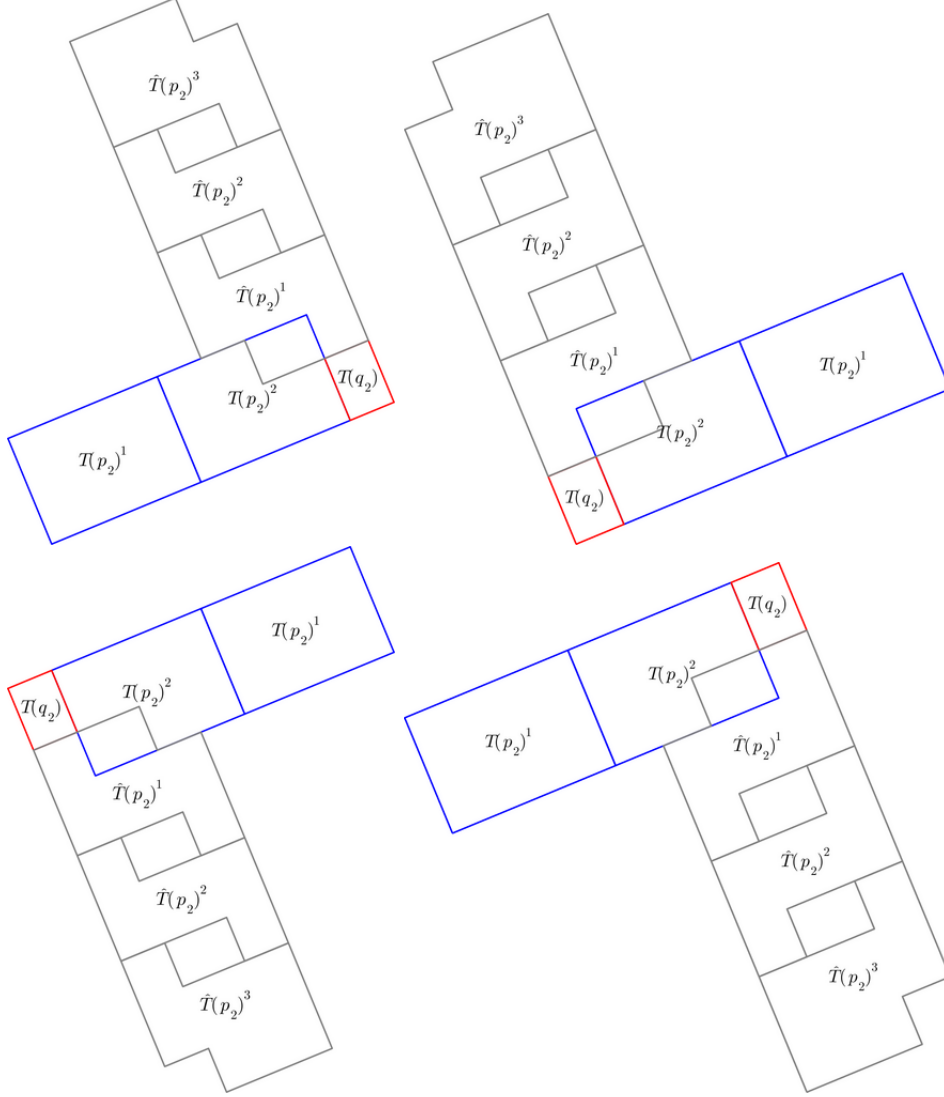


FIGURE 26. The four possible orientations for an even L -correction as described in Definition 11. From top left to bottom right, 10, 00, 11 then 01.

9. GLOBAL ODOMETERS

We now observe that both weak and alternate tile odometers can be extended to global odometers with the correct growth.

Lemma 9.1. *For every reduced fraction $0 < n/d < 1$, there are two functions, g, \hat{g} on \mathbb{Z}^2 whose restriction to a standard or alternate tile are alternate and standard tile odometers for which the periodicity condition 9 holds and for which*

$$(70) \quad x \rightarrow f(x) - \frac{1}{2}x^t M(n, d)x - b \cdot x$$

is $L'(n/d)$ -periodic for some $b \in \mathbb{R}^2$, for each $f \in \{g, \hat{g}\}$.

Proof. Given that we have proved standard and alternate tile odometers which are lattice adjacent are compatible, the proof is identical to Lemma 10.1 in [LPS16]. \square

- [BTW87] Per Bak, Chao Tang, and Kurt Wiesenfeld. Self-organized criticality: An explanation of the $1/f$ noise. *Physical review letters*, 59(4):381, 1987.
- [CP18] Scott Corry and David Perkinson. *Divisors and sandpiles*, volume 114. American Mathematical Soc., 2018.
- [CPS08] Sergio Caracciolo, Guglielmo Paoletti, and Andrea Sportiello. Explicit characterization of the identity configuration in an abelian sandpile model. *Journal of physics A: mathematical and theoretical*, 41(49):495003, 2008.
- [Dha90] Deepak Dhar. Self-organized critical state of sandpile automaton models. *Physical Review Letters*, 64(14):1613–1616, 1990.
- [DS10] Deepak Dhar and Tridib Sadhu. Pattern formation in growing sandpiles with multiple sources or sinks. *Journal of Statistical Physics*, 138(4-5):815–837, 2010.
- [DS11] Deepak Dhar and Tridib Sadhu. The effect of noise on patterns formed by growing sandpiles. *Journal of Statistical Mechanics: Theory and Experiment*, 2011(03):P03001, 2011.
- [DS13] Deepak Dhar and Tridib Sadhu. A sandpile model for proportionate growth. *Journal of Statistical Mechanics: Theory and Experiment*, 2013(11):P11006, 2013.
- [DSC09] Deepak Dhar, Tridib Sadhu, and Samarth Chandra. Pattern formation in growing sandpiles. *EPL (Europhysics Letters)*, 85(4):48002, 2009.
- [GLM⁺05] Ronald L Graham, Jeffrey C Lagarias, Colin L Mallows, Allan R Wilks, and Catherine H Yan. Apollonian circle packings: geometry and group theory i. the apollonian group. *Discrete & Computational Geometry*, 34(4):547–585, 2005.
- [HLM⁺08] Alexander E Holroyd, Lionel Levine, Karola Mészáros, Yuyal Peres, James Propp, and David B Wilson. Chip-firing and rotor-routing on directed graphs. In *In and out of equilibrium 2*, pages 331–364. Springer, 2008.
- [Jár18] Antal A Járai. Sandpile models. *Probability surveys*, 15:243–306, 2018.
- [KK21] Michael Kapovich and Alex Kontorovich. On superintegral kleinian sphere packings, bugs, and arithmetic groups. *arXiv preprint arXiv:2104.13838*, 2021.
- [Kli18] Caroline J Klivans. *The mathematics of chip-firing*. CRC Press, 2018.
- [LBR02] Yvan Le Borgne and Dominique Rossin. On the identity of the sandpile group. *Discrete mathematics*, 256(3):775–790, 2002.
- [LKG90] SH Liu, Theodore Kaplan, and LJ Gray. Geometry and dynamics of deterministic sand piles. *Physical Review A*, 42(6):3207, 1990.
- [LP10] Lionel Levine and James Propp. What is... a sandpile. In *Notices Amer. Math. Soc*, 2010.
- [LPS16] Lionel Levine, Wesley Pegden, and Charles K Smart. Apollonian structure in the abelian sandpile. *Geometric and Functional Analysis*, 26(1):306–336, 2016.
- [LPS17] Lionel Levine, Wesley Pegden, and Charles K Smart. The apollonian structure of integer superharmonic matrices. *Annals of Mathematics*, pages 1–67, 2017.
- [Mel20] Andrew Melchionna. The sandpile identity element on an ellipse. *arXiv preprint arXiv:2007.05792*, 2020.
- [Ost03] Srdjan Ostojic. Patterns formed by addition of grains to only one site of an abelian sandpile. *Physica A: Statistical Mechanics and its Applications*, 318(1-2):187–199, 2003.
- [Pao12] Guglielmo Paoletti. Deterministic abelian sandpile models and patterns. 2012.
- [Peg] Wesley Pegden. Sandpile galleries. <http://www.math.cmu.edu/~wes/sandgallery.html>.
- [PS13] Wesley Pegden and Charles Smart. Convergence of the abelian sandpile. *Duke mathematical journal*, 162(4):627–642, 2013.
- [PS20] Wesley Pegden and Charles K Smart. Stability of patterns in the abelian sandpile. In *Annales Henri Poincaré*, volume 21, pages 1383–1399. Springer, 2020.
- [Red05] Frank Redig. Mathematical aspects of the abelian sandpile model. *Les Houches lecture notes*, 83:657–659, 2005.
- [Sma13] Charles K Smart. Aim chip firing 2013: The f -lattice. 2013. <https://www.aimath.org/WWN/chipfiring/flattice.pdf>.
- [Tan96] Lin Tan. The group of rational points on the unit circle. *Mathematics Magazine*, 69(3):163–171, 1996.